國 立 交 通 大 學

電 機 與 控 制 工 程 學 系

碩 士 論 文

以頻域為基準之時域等化器運用於數位用戶迴路之設計

A Frequency Domain Based TEQ Design for DSL Systems

研 究 生：林 裕 彬

指 導 教 授：林 源 倍 博士

中華民國九十四年七月

以頻域為基準之時域等化器運用於數位用戶迴路之設計

A Frequency Domain Based TEQ Design for DSL Systems

研 究 生 : 林 裕 彬　　Student:Yu-Pin Lin

指導教授 : 林源倍博士　Advisor:Dr. Yuan-Pei Lin

國 立 交 通 大 學

電 機 與 控 制 工 程 學 系

A Thesis
Submitted to institute of Electrical and Control Engineering
College of Electrical Engineering and Information Science
National Chiao Tung University
In Partial Fulfillment of the Requirements
for the Degree of Master
In
Electrical and Control Engineering
July 2005
Hsinchu, Taiwan, Republic of China
中華民國九十四年七月

以頻域為基準之時域等化器運用於數位用戶迴路之設計

研究生 ： 林裕彬　　指導教授 ： 林源倍博士

國立交通大學電機與控制工程學系(研究所)碩士班

摘 要

離散多調(DMT)已經成功應用於數位用戶迴路(DSL)上。在數位用戶迴路的應用上,通道長度太長時,會加入時域等化器(TEQ)來縮短等效通道長度並降低干擾。另外,等化過後通道的頻率響應對傳輸率也有重要的影響。特別是當零點發生在傳輸頻帶時,會造成傳輸率的下降。在論文中, 我們提出一個以頻域為基準的等化器設計方法來降低頻率上的干擾。這個方法考慮到了等化過後通道的頻率響應。最後,我們模擬極高速數位用戶迴路(VDSL)來說明這個方法的效果。從模擬可以看出這個等化器可以有效地改善傳輸率。

A Frequency Domain Based TEQ Design for DSL Systems

Student : Yu-Pin Lin Advisor : Yuan-Pei Lin

Department of Electrical and Control Engineering
National Chiao Tung University

Abstract

The Discrete MultiTone system has been successfully applied to Digital Subscriber Lines (DSL) system. For DSL applications, the channels length are generally very long and a Time Domain Equalizer (TEQ) is usually used to shorten the effective channel and mitigate interference. On the other hand, the frequency response of the equalized channel is crucial for determining transmission bit rate. In particular, zeros in the transmission bands often results in a loss in bit rate. In this thesis, we proposed a novel frequency domain based TEQ design. Interference is minimized in the frequency domain. This method takes into account the frequency response of the equalized channel implicitly. We will use Very-high speed Digital Subscriber Line system as an example to demonstrate the usefulness of the proposed method. Simulation examples show that the frequency domain based TEQ have very good bit rate.

致謝

論文中的 TEQ 設計方法在三、四月時，仍在修改當中。當時的心情真是忐忑不安。在許多未知的途徑摸索，如果沒有林源倍老師的循循善誘。不知道要花費多少時間在無用的方法上轉。老師不厭其煩的指導，看在資質駑鈍的我的眼中，除了敬佩還帶了三分慚愧。不過這些努力現在有了這個小小的成果。

同時也感謝口試委員吳炳飛，林清安及鄭木火教授在百忙之中抽空給予指導與建議，使本文更加完備。

國輝及孟良學長在週末時，陪我到郊外踏青或運動。禮涵學長給予我程式模擬的建議。實驗室的各位同門，在我每晚挑燈夜戰前，一起走去買宵夜。父母家人的支持以及許多朋友對我的幫助。都是在這段日子必須提到的正面幫助。願這些人將來都能順利。加油。

林裕彬 謹誌

Contents

List of Figures

List of Tables

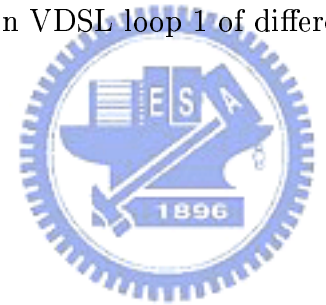

Chapter 1

Introduction

The Discrete Fourier Transform (DFT) based Discrete MultiTone (DMT) transceiver has found important applications in Digital Subscriber Line (DSL), [1]-[2]. The transmitter and receiver perform respectively M-point Inverse Discrete Fourier Transform (IDFT) and DFT computation, where M is the number of tones or number of sub-channels. At the transmitter end, each block is padded with a Cyclic Prefix (CP) of length L. If L is no smaller than the order of the channel ν, then the Inter-Block Interference (IBI) can be removed easily by discarding the prefix at the receiver. As a result, an finite impulse response (FIR) channel is converted into M frequency non-selective parallel sub-channels. The sub-channel gains are the M-point DFT of the channel impulse response. When the channel is longer or much longer than L, which is usually the case in DSL applications, a Time domain EQualizer (TEQ) is usually inserted at the receiver to shorten the channel impulse response so that the equalized channel has most of the energy concentrated in a window of $L+1$ samples [3]. The samples outside the window, however, will lead to IBI, which reduces Signal to Interference and Noise Ratio (SINR) and thus affects transmission bit rate. The TEQ plays an important role in the application of Discrete MultiTone (DMT) to DSL [1]-[2]. The bit rate that can be transmitted are greatly affected by the design of TEQ.

If $\nu+1$ is larger than L, Inter-Symbol Interference (ISI) is raised to disturb the transmitted signal. To combat the ISI, we will introduce TEQ to shorten the equalized channel, which is the channel convolving the TEQ, within a length

$L+1$ window. Then, the energy of the equalized channel outside the window is reduced and ISI power is eliminated. In Melsa's earlier work [3], he proposed a TEQ, called Maximized the Shortening SNR (MSSNR), to maximize the energy inside the window to energy outside the window ratio and exhaustively search the optimal start point of window which the ratio is largest than others. This solution of the cost function is an eigenvalue problem and channel coefficients shall be known, it provides an optimal design method to maximize Signal to Interference Ratio (SIR). For the solution is easily computed and optimal SIR, this TEQ will be the benchmark to compare with other methods.

Differing from MSSNR method, the "Multicarrier Equalization by Restoration of RedundancY" (MERRY) algorithm is a blind channel shortening method [4]. This method uses the property of CP. If the channel length is smaller than CP length and due to the CP is the repeat the last L samples in DMT symbol, The receiving sequence where location corresponding to the CP shall match the last samples. MERRY algorithm is to minimize the mean square error of some samples in the position corresponding to CP and the last samples in an adaptive way, then, channel shortening is achieved.

A semi-blind method to combat the ISI was proposed in [5], we called it MFSIR in our thesis. This method needs not know the channel impulse response. DSL systems use Frequency Division Duplexing (FDD) to separate upstream and downstream and the null tones does not be assigned bit. In training phase, the pilot tones are assigned the same Quadrature Amplitude Modulation (QAM) symbol every DMT blocks. We can collect the output signals of FFT block in the DMT system corresponding to the null tones and take average on them. The averaged output signals will have nothing but interference if the channel order is larger than CP length. When we cumulate large number of the output signals, the power of pilot tones and the power of null tones interference can be obtained. MFSIR design a TEQ maximizing the power of pilot tones to the null tones interference power. This optimal problem can be solved as a eigen problem.

In the "Sum-square Auto-correlation Minimization" (SAM) algorithm [6], the autocorrelation function of channel $R_{cc}[n]$ will be zero $\forall n > L$ as channel length $<$

$L+1$, SAM algorithm is to minimize the power of $R_{cc}[n]$ $\forall n > L$. SAM algorithm shall meet some conditions to be appropriate for DMT system, the author argued the reasons and provided an example of Asymmetric Digital Subscriber Line (ADSL) system to show SAM is appropriate for DMT system.

The methods mentioned above are designed for combating the ISI, the bit rate performance will be improved as the ISI be eliminated. But the bit rate and ISI have no direct relations. A method to design TEQ for maximizing bit rate is proposed in [7] where the summation of used tones SINR is obtained. To maximize the SINR is a nonlinear optimal problem and the convergence is not guaranteed. In [8], a method design TEQ for each used tones for maximizing the individual tone SINR. This method is also in the bit rate maximizing sense. There are k_u cost functions to be solved where k_u is the number of used tones. Although each cost function is easily solved by a eigen problem. There are k_v TEQ to be implemented, it is too large complexity to implement. There are still many algorithm [11] [12] to improve the DMT system performance, for comparison in our simulations, MSSNR, MERRY and MFSIR cost function will be derived in following section.

On the other hand, the frequency response of the equalized channel is crucial for determining transmission bit rate. DSL systems use FDD to separate upstream and downstream transmission. If a zeros in the transmission bands, the signal power will be down and resulting in a loss in bit rate. In this thesis, we proposed a novel frequency domain based TEQ design. Some tones Interference form other tones are minimized in the frequency domain. And observing the equalized channel and magnitude response of TEQ, we will give a scheme to shorten the equalized channel and avoid zeros of TEQ being in the transmission bands. This method takes into account the frequency response of the equalized channel implicitly.

The goal of above TEQ design is to shorten the channel, furthermore, reduce the interference. Interference is smaller than noise in short loop length and getting larger as loop length longer. In short loop length channel, TEQ is not important for the bit rate performance. For long loops, the TEQ significant enhances the

bit rate performance.

Outline

In Chapter 2, we will derive equivalent discrete time channel with Discrete to Continuous (D/C) and Continuous to Discrete (C/D) converter and the statistical properties of D/C and C/D converter. The surveys of MSSNR and MERRY TEQ algorithm will be presented for comparison with our proposed TEQ design in Chapter 4. The proposed TEQ design method will be given in Chapter 5. Numerical simulations and TEQ performance comparisons will be presented in Chapter 6. A conclusion is given in Chapter 7.

1.1 Notations

- Boldfaced lower case letters represent vectors and boldfaced upper letters are reserved for matrices. The notation $\mathbf{A}^{\dagger}$ denotes transpose-conjugate of $\mathbf{A}$.

- M is the DFT size, L is the cyclic prefix length, $N = M + L$ is the symbol size, T is the sampling period, ν is the channel order, T_e is the TEQ length, d is the synchronization delay. The notation $*$ represents convolution operator and c^* means complex conjugate of c.

- The notation $\mathbf{W}$ is used to represent the unitary DFT matrix whose elements given by,

$$W_{kn} = \frac{1}{\sqrt{M}} e^{-j\frac{2\pi}{M}kn} \quad for \quad 0 \leq k, n \leq M-1$$

- The notation $\mathbf{I}_K$ is used to represent a $K \times K$ identity matrix.

Chapter 2

Transceivers with D/C and C/D

A complete communication system usually includes D/C and C/D operations. At the transmitter, bit stream to be transmitted is mapped to modulation symbols, which, possibly after some processing, is converted to an analog signal and sent to the channel. At the receiver, an analog received signal is first converted to digital signal before further processing. In this chapter, we will first present the equivalent discrete time channel in Section 2.1. Statistical properties of D/C and C/D will be given in Section 2.2 and 2.3, respectively.

2.1 Equivalent Discrete Time Channel

A D/C converter and its equivalent block diagram is shown in Figure 2.1. A D/C converter can be viewed as the interconnection of 2 blocks. The first block converts a discrete time sequence to a continuous time signal $x_s(t)$ of impulse train with impulses separated by an underlying period T. The signal $x_s(t)$ can be expressed as

$$x_s(t) = \sum_{n=-\infty}^{\infty} s[n]\delta(t - nT). \tag{2.1}$$

The second one is the reconstruction filter $h_r(t)$. The output reconstructed continuous time signal $x(t)$ is given by,

$$x(t) = \sum_{n=-\infty}^{\infty} s[n]h_r(t - nT). \tag{2.2}$$

For a C/D converter shown in Figure 2.2.(a), the output discrete sequence

$y[n]$ is related to the input continuous time signal $r(t)$ by $y[n] = r(nT)$. Usually a antialiasing filter $h_a(t)$ is included before C/D as shown in Figure 2.2.(b) to obtain a bandlimited waveform $a(t)$. In this case, we have

$$\begin{aligned} a(t) &= r(t) * h_a(t) \\ y[n] &= a(nT) = (r(t) * h_a(t))|_{t=nT}. \end{aligned} \tag{2.3}$$

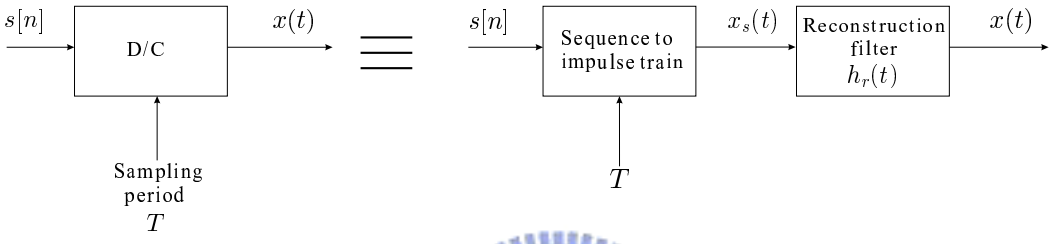

Figure 2.1: The block diagram of a D/C converter.

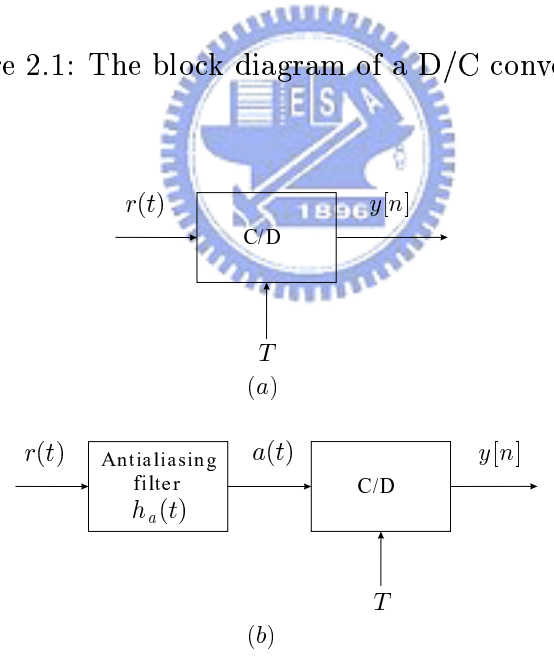

Figure 2.2: (a) The block diagram of a C/D converter, (b) a C/D converter with antialaising filter.

Convolving the reconstruction filter $h_r(t)$, continuous channel $h(t)$ and the antialiasing filter $h_a(t)$ in Figure 2.3, we have

$$c(t) = h_r(t) * h(t) * h_a(t).$$

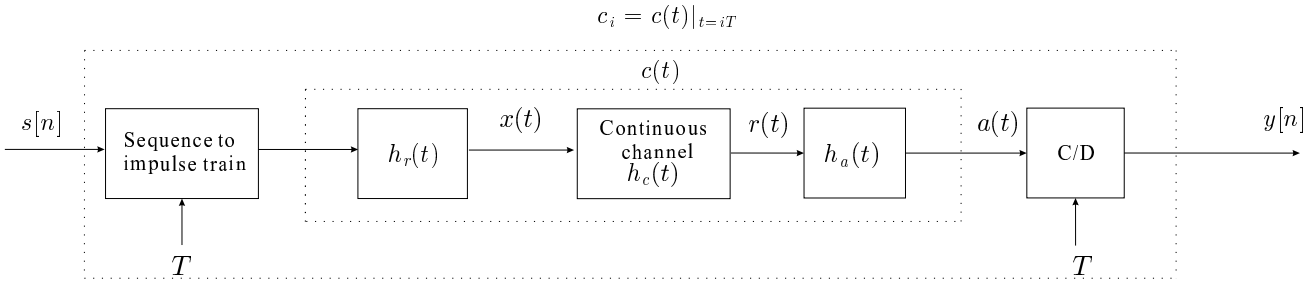

Figure 2.3: Continuous-time processing represented as discrete-time equivalent channel.

The equivalent discrete time channel is

$$c_i = c(t)|_{t=iT}.$$

Assume the D/C is ideal reconstruction, $X(j\Omega)$ and $A(j\Omega)$ will be zeros for $|\Omega| > \pi/T$. Thus, $A(j\Omega)$ is no aliasing. The output of D/C and C/D converter can be expressed as

$$x(t) = \sum_{n=-\infty}^{\infty} s[n] \frac{sin[\pi(t-nT)/T]}{\pi(t-nT)/T} \tag{2.4}$$

and

$$a(t) = \sum_{n=-\infty}^{\infty} y[n] \frac{sin[\pi(t-nT)/T]}{\pi(t-nT)/T} \tag{2.5}$$

The frequency domain relationship for Figure 2.3 are

$$\begin{aligned} X(j\Omega) &= \int_{-\infty}^{\infty} \sum_{n=-\infty}^{\infty} s[n] h_r(t-nT) e^{-j\Omega t} dt \\ &= \sum_{n=-\infty}^{\infty} s[n] H_r(j\Omega) e^{-j\Omega T n} = H_r(j\Omega) S(e^{j\Omega T}) \\ &= T S(e^{j\Omega T}) \quad |\Omega| < \pi/T, \end{aligned} \tag{2.6}$$

$$A(j\Omega) = H_a(j\Omega) \cdot H_c(j\Omega) \cdot X(j\Omega) \quad |\Omega| < \pi/T, \tag{2.7}$$

$$Y(e^{j\omega}) = \frac{1}{T} A(j\frac{\omega}{T}) \quad |\omega| < \pi. \tag{2.8}$$

From Equation 2.6, 2.7 and 2.8, the overall system can be modeled as a equivalent discrete time channel, c_i, and the frequency response of c_i is

$$C(e^{j\omega}) = H_a(j\frac{\omega}{T}) \cdot H_c(j\frac{\omega}{T}) \quad |\omega| < \pi. \tag{2.9}$$

2.2 Statistical Properties of D/C Converter

In this section, we will derive the PSD of input signal $s[n]$ and output signal $x(t)$ of the D/C process, the detail is in Subsection 4.4.1 of [10]. Suppose the input sequence $s[n]$ is Wide Sense Stationary (WSS) with autocorrelation function $R_s[k]$ and mean m_s. From Equation 2.2, the autocorrelation of $x_r(t)$ is

$$\begin{aligned} R_x(t, t+\tau) &= E[x(t)x(t+\tau)] \\ &= \sum_{n=-\infty}^{\infty} \sum_{m=-\infty}^{\infty} E[s[n]s[m]]h_r(t-nT)h_r(t+\tau-mT), \quad (let\ m-n=k) \\ &= \sum_{k=-\infty}^{\infty} R_s[k] \sum_{n=-\infty}^{\infty} h_r(t-nT)h_r(t+\tau-kT-nT). \end{aligned} \tag{2.10}$$

We can verify that $x_c(t)$ is a Wide CycloStationary Sense (WCSS) process, that is,

$$\begin{aligned} E[x(t+T)] &= E[x(t)] \\ R_x(t+T, t+\tau+T) &= R_x(t, t+\tau). \end{aligned} \tag{2.11}$$

The mean and autocorrelation function are periodic function with period T. The PSD of the WCSS process $x(t)$ is a two dimension Fourier transform of $R_x(t, t+\tau)$. It depends on two variable t and τ. The time average autocorrelation function is

$$\begin{aligned} \overline{R}_x(\tau) &= \frac{1}{T} \int_{\frac{-T}{2}}^{\frac{T}{2}} R_x(t, t+\tau)dt \\ &= \sum_{k=-\infty}^{\infty} R_s[k] \sum_{n=-\infty}^{\infty} \frac{1}{T} \int_{\frac{-T}{2}}^{\frac{T}{2}} h_r(t-nT)h_r(t+\tau-kT-nT)dt \\ &= \sum_{k=-\infty}^{\infty} R_s[k] \sum_{n=-\infty}^{\infty} \frac{1}{T} \int_{\frac{-T}{2}-nT}^{\frac{T}{2}-nT} h_r(t)h_r(t+\tau-kT)dt. \end{aligned} \tag{2.12}$$

We define the deterministic autocorrelation of h_r as

$$R_{h_r}(\tau) = \int_{-\infty}^{\infty} h_r(t)h_r(t+\tau)dt.$$

Then Equation 2.12 can be expressed as

$$\overline{R}_x(\tau) = \frac{1}{T}\sum_{k=-\infty}^{\infty} R_s[k]R_{h_r}(\tau - kT). \tag{2.13}$$

The average PSD of $x(t)$ is defined as the Fourier transform $\overline{R}_x(\tau)$.

$$\begin{aligned}
\overline{S}_x(j\Omega) &= \frac{1}{T}\int_{-\infty}^{\infty}\sum_{k=-\infty}^{\infty} R_s[k]R_{h_r}(\tau - kT)e^{-j\Omega\tau}d\tau \\
&= \frac{1}{T}\sum_{k=-\infty}^{\infty} R_s[k]e^{-j\Omega Tk}|H_r(j\Omega)|^2 \\
&= \frac{1}{T}S_s(e^{j\Omega T})|H_r(j\Omega)|^2. \qquad (2.14)
\end{aligned}$$

We can conclude that the output of D/C converter is a continuous WSCS process when the input is a discrete WSS process. From Equation 2.14, we have the relation between PSD of $s[n]$ and average PSD of $x(t)$. The mean square of $x(t)$, i.e., $E[x^2(t)]$ can be obtained from $\overline{S}_x(j\Omega)$ using

$$E[x^2(t)] = \int_{-\infty}^{\infty} \overline{S}_x(j\Omega)d\Omega.$$

If the sequence is white, then $R_x[k] = R_x[0]\delta[k]$ and $E[x^2(t)] = \frac{R_x[0]}{T}\int_{-\infty}^{\infty}|H_r(j\Omega)|^2 d\Omega$. The signal $x(t)$ is a voltage signal and measured across a terminated resistor R_v. Then the measured PSD at the output of D/D converter can be expressed as

$$\overline{S}_x(j\Omega)/R_v \quad (Watt/Hz).$$

2.3 Statistical Properties of C/D Converter

Suppose the input signal $r(t)$ is WSS with autocorrelation function $R_r(\tau)$ and mean m_r. The autocorrelation function of the discrete sequence is

$$E[y[n]y[m]] = E[r(nT)r(mT)] = R_r((m-n)T).$$

The autocorrelation function of $y[n]$ can be obtained by simply sampling the autocorrelation function of $r(t)$. Also the mean function of $y[n]$ is

$$E[y[n]] = E[r(nT)] = m_r,$$

i.e., $m_y = m_r$ and therefore the discrete time sequence $y[n]$ is also WSS with autocorrelation function $R_y[k] = R_r(kT)$. The PSD of $y[n]$ is

$$S_y(e^{j\omega}) = \frac{1}{T}\sum_{n=-\infty}^{\infty} S_r(j(\frac{\omega - 2\pi n}{T})). \tag{2.15}$$

In practice, an antialiasing filter $h_a(t)$ is included before the C/D converter as shown in Figure 2.2(b). In this case, we have

$$\begin{aligned} S_y(e^{j\omega}) &= \frac{1}{T}\sum_{n=-\infty}^{\infty} S_a(j(\frac{\omega - 2\pi n}{T})) \\ &= \frac{1}{T}\sum_{n=-\infty}^{\infty} S_r(j(\frac{\omega - 2\pi n}{T}))|H_a(j\frac{\omega}{T})|^2. \end{aligned} \tag{2.16}$$

Chapter 3

DMT System

3.1 DMT System Model

The block diagram of a DMT system is shown in Figure 3.1. The channel is modeled as continuous time LTI filter $h_c(t)$ plus noise $n(t)$. The input is a $M \times 1$ vector $\mathbf{s}[i]$, consisting of QAM modulation symbols, where M is the number of sub-channels. Each input vector is passed through an $M \times M$ IDFT matrix. The P/S operation (parallel to serial conversion) converts each $M \times 1$ vector into M serial samples. The Cyclic Prefix (CP) operation adds a CP of length L to each block. The output sequence g_i is sent to the D/C converter and to the channel $h_c(t)$. At the receiver, the received signal $v(t)$ is first sampled. For the received discrete time sequence, prefix is removed and Serial to Parallel (S/P) operation is performed to convert the sequence to $M \times 1$ vector $\mathbf{y}[i]$. An appropriate delay d is included for symbol synchronization before CP removal. For the convenience of formulation, the value of d is allowed to lie positive. This does not affect actual implementation. Finally, DFT is applied on each $\mathbf{y}[i]$ to obtain the receiver output vector $\mathbf{u}[i]$.

From g_i, the input of the D/C at the transmitter, to v_i output of the C/D at the receiver, we can represent it as a equivalent discrete time channel model as we did in section 2.1. The resulting DMT system block diagram is as shown in Figure 3.2. To have real transmission signal g_i, the modulation symbols in the input vector $\mathbf{s}[i]$ are not completely free. In particular, for real g_i, $\mathbf{s}[i]$ need to

have the conjugate symmetric property, $s_k[i] = s^*_{M-k}[i]$.

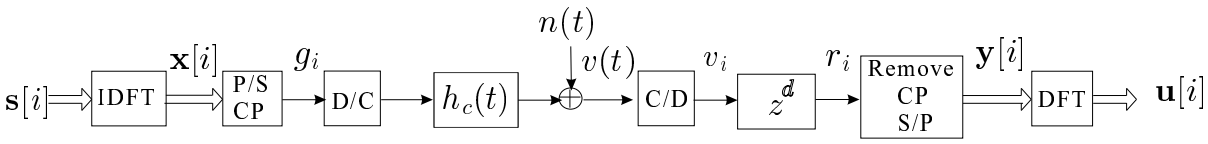

Figure 3.1: DMT system block diagram.

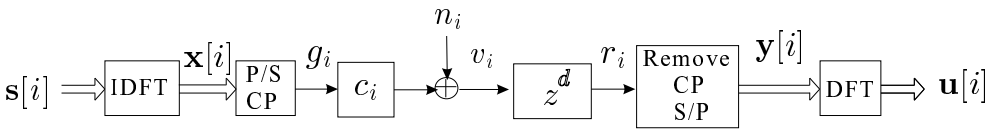

Figure 3.2: DMT system block diagram with equivalent discrete time channel.

Matrix Representation. The vector $\mathbf{x}[i]$ in Figure 3.2 passed through the cyclic prefix and P/S blocks to be a sequence g_i. The P/S block can be implemented using expander and delays as shown in Figure 3.3. We can collect N samples of g_i to form a $N \times 1$ vector $\mathbf{g}[i]$

$$g_k[i] \quad = \quad g_{iN+k}, \tag{3.1}$$

where $g_k[i]$ is the k-th elements of vector $\mathbf{g}[i]$. The relationship of $\mathbf{g}[i]$ and $\mathbf{x}[i]$ is

$$\mathbf{g}[i] = \begin{bmatrix} x_{M-L}[i] \\ \vdots \\ x_{M-1}[i] \\ x_0[i] \\ \vdots \\ x_{M-1}[i] \end{bmatrix} = \begin{bmatrix} \mathbf{0} & \mathbf{I}_L \\ & \mathbf{I}_M \end{bmatrix} \mathbf{x}[i], \tag{3.2}$$

and define

$$\mathbf{F}_0 \quad = \quad \begin{bmatrix} \mathbf{0} & \mathbf{I}_L \\ & \mathbf{I}_M \end{bmatrix}. \tag{3.3}$$

The sequence r_i in Figure 3.2 is $r_i = c_i * g_{i+d} + n_{i+d}$, i.e.,

$$r_i = \sum_{k=0}^{N-1} c_k * g_{i-k+d} + n_{i+d} \tag{3.4}$$

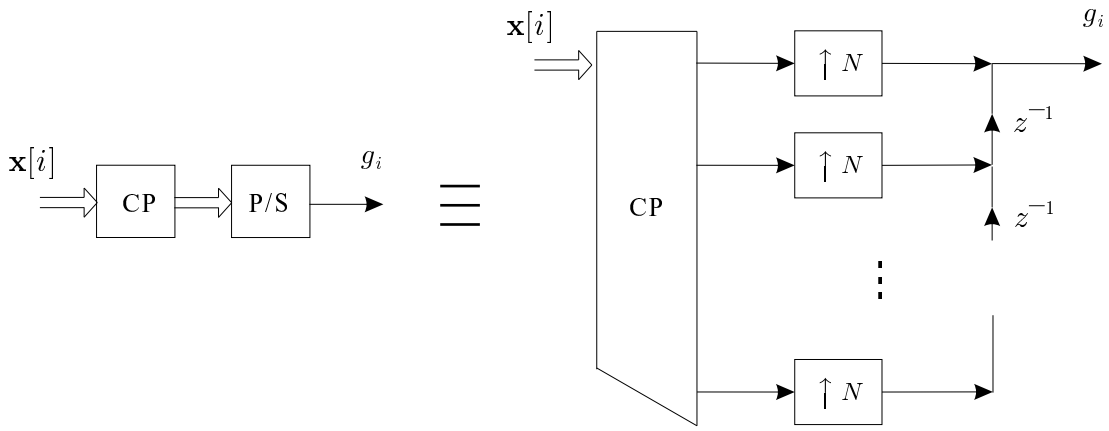

Figure 3.3: The representation of P/S block using expanders and delays.

This can be written in matrix form.

$$\begin{bmatrix} r_{iN} \\ r_{iN+1} \\ \vdots \\ r_{iN+N-1} \end{bmatrix} = \begin{bmatrix} c_d & \cdots & c_0 & 0 & \cdots & 0 \\ \vdots & & & & \ddots & \vdots \\ c_{N-1} & & \ddots & & & 0 \\ 0 & & & & & c_0 \\ \vdots & \ddots & & & \ddots & \vdots \\ 0 & \cdots & 0 & c_{N-1} & \cdots & c_d \end{bmatrix} \begin{bmatrix} z_{iN} \\ z_{iN+1} \\ \vdots \\ z_{iN+N-1} \end{bmatrix}$$

$$+ \begin{bmatrix} 0 & \cdots & c_{N-1} & \cdots & c_{d+1} \\ \vdots & & & \ddots & \vdots \\ & \ddots & & & c_{N-1} \\ \vdots & \ddots & & \ddots & \vdots \\ 0 & \cdots & & \cdots & 0 \end{bmatrix} \begin{bmatrix} z_{(i-1)N} \\ z_{(i-1)N+1} \\ \vdots \\ z_{(i-1)N+N-1} \end{bmatrix}$$

$$+ \begin{bmatrix} 0 & \cdots & & \cdots & 0 \\ \vdots & & & \ddots & \vdots \\ c_0 & \ddots & & & 0 \\ \vdots & \ddots & & \ddots & \vdots \\ c_{d-1} & \cdots & c_0 & \cdots & 0 \end{bmatrix} \begin{bmatrix} z_{(i+1)N} \\ z_{(i+1)N+1} \\ \vdots \\ z_{(i+1)N+N-1} \end{bmatrix} + \begin{bmatrix} n_{iN+d} \\ n_{iN+d+1} \\ \vdots \\ n_{iN+d+N-1} \end{bmatrix}$$

$$= \mathbf{C}_0\mathbf{g}[i] + \mathbf{C}_1\mathbf{g}[i-1] + \mathbf{C}_2\mathbf{g}[i+1] + \mathbf{n}[i]. \tag{3.5}$$

Let's define the block $\mathbf{C}(z)$ as

$$\mathbf{C}(z) = \mathbf{C}_0 + z^{-1}\mathbf{C}_1 + z\mathbf{C}_2, \tag{3.6}$$

to represent the operations of convolution with equivalent channel and the synchronization delay. $\mathbf{C}_0$ represents the amplitude of transmitted symbol $\mathbf{s}[i]$ and brings the Inter Carrier Interference (ICI), $\mathbf{C}_1$ and $\mathbf{C}_2$ bring the Inter Block Interference (IBI). The input of remove CP and S/P block r_i is a serial sequence and be discarded the guard band and collected to an $M \times 1$ vector $\mathbf{y}[i]$, the relationship of the input and output can be expressed as

$$\begin{bmatrix} y_0[i] \\ y_1[i] \\ y_{M-1}[i] \end{bmatrix} = \begin{bmatrix} r_{L+1}[i] \\ r_{L+2}[i] \\ \vdots \\ r_{N-1}[i] \end{bmatrix} = [\,\mathbf{0} \quad \mathbf{I}_M\,]\,\mathbf{r}[i], \tag{3.7}$$

and define

$$\mathbf{F}_1 = [\,\mathbf{0} \quad \mathbf{I}_M\,]\,. \tag{3.8}$$

From the derivations of Equations 3.2, 3.5 and 3.7, the operations in Figure 3.2 can be represented as matrix operations and redrawn in Figure 3.4. From the matrix representation, the received output vector $\mathbf{u}[i]$ can be represented as

$$\begin{aligned} \mathbf{u}[i] &= \underbrace{\mathbf{W}\mathbf{F}_1\mathbf{C}_0\mathbf{F}_0\mathbf{W}^\dagger}_{\mathbf{B}_0}\mathbf{s}[i] + \underbrace{\mathbf{W}\mathbf{F}_1\mathbf{C}_1\mathbf{F}_0\mathbf{W}^\dagger}_{\mathbf{B}_1}\mathbf{s}[i-1] + \underbrace{\mathbf{W}\mathbf{F}_1\mathbf{C}_2\mathbf{F}_0\mathbf{W}^\dagger}_{\mathbf{B}_2}\mathbf{s}[i+1] + \underbrace{\mathbf{W}\mathbf{F}_1\mathbf{n}[i]}_{\mathbf{e}[i]} \\ &= \mathbf{B}_0\mathbf{s}[i] + \mathbf{B}_1\mathbf{s}[i-1] + \mathbf{B}_2\mathbf{s}[i+1] + \mathbf{W}\mathbf{F}_1\mathbf{e}[i]. \end{aligned} \tag{3.9}$$

If the channel order ν is smaller than L and synchronization delay d is zero, we have

$$\mathbf{B}_1 = \mathbf{B}_2 = \mathbf{0}, \tag{3.10}$$

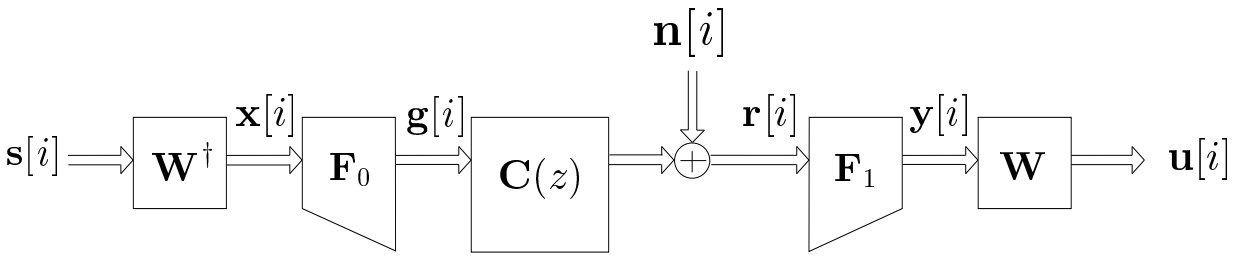

Figure 3.4: DMT matrix representation.

and

$$\mathbf{F}_1\mathbf{C}_0(z)\mathbf{F}_0 = \begin{bmatrix} c_0 & 0 & \cdots & 0 & c_L & \cdots & c_1 \\ c_1 & c_0 & \ddots & & 0 & \ddots & \vdots \\ \vdots & & \ddots & & & \ddots & c_L \\ c_L & c_{L-1} & & c_0 & 0 & & 0 \\ 0 & c_L & & & \ddots & & \vdots \\ \vdots & \ddots & \ddots & & & \ddots & 0 \\ 0 & \cdots & 0 & c_L & c_{L-1} & \cdots & c_0 \end{bmatrix}_{M\times M} \triangleq \mathbf{C}_{cir}. \tag{3.11}$$

The matrix $\mathbf{C}_{cir}$ is independent of z, then, the IBI vanishes, and $\mathbf{C}_{cir}$ is a circulant matrix. It is known that circulant matrices can be diagonalized using DFT matrices,

$$\mathbf{W}\mathbf{C}_{cir}\mathbf{W}^{\dagger} = \mathbf{\Lambda}, \tag{3.12}$$

where $\mathbf{\Lambda}$ is a diagonal matrix with diagonal elements C_k, which are the M-point DFT of channel coefficients $c_0, c_1 \cdots c_L$, In this case the whole system can be considered as M parallel sub-channels as shown in figure 3.5.

If the channel order is larger than L, usually the case in DSL applications, a TEQ is introduced to shorten the channel. In Figure 3.6, a TEQ is included in the DMT system, Let $h_i = c_i * t_i$ be the effective channel impulse response. Similar to the above derivation, the overall system can be represented using matrix representation as shown in Figure 3.7. The matrix $\mathbf{H}(z)$ is given by

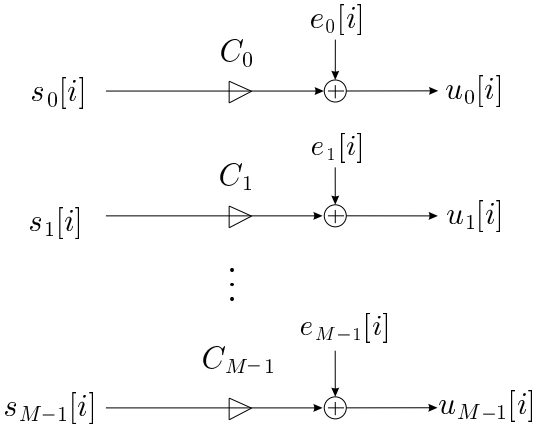

Figure 3.5: Equivalent M parallel sub-channels.

$$\mathbf{H}(z) = \begin{bmatrix} h_d & \cdots & \cdots & h_0 & z^{-1}h_{N-1} & \cdots & z^{-1}h_{d+1} \\ \vdots & \ddots & & & & \ddots & \vdots \\ \vdots & & & & & \ddots & z^{-1}h_{N-1} \\ h_{N-1} & & & \ddots & & & h_0 \\ zh_0 & \ddots & & & & & \vdots \\ \vdots & \ddots & \ddots & & & \ddots & \vdots \\ zh_{d-1} & \cdots & zh_0 & h_{N-1} & \cdots & \cdots & h_d \end{bmatrix}_{N\times N}. \quad (3.13)$$

The derivation of Equation 3.13 is similar to that of Equation 3.5. If the channel order is larger than prefix length L, received symbol will be affected by ISI. From matrix representation, the equalized channel matrix $\mathbf{H}(z)$ can be expressed as

$$\mathbf{H}(z) = \mathbf{H}_0 + z^{-1}\mathbf{H}_1 + z\mathbf{H}_2, \quad (3.14)$$

where $\mathbf{H}_0$, $\mathbf{H}_1$, and $\mathbf{H}_2$ are independent of z. The relationship between input signal vector $\mathbf{s}[i]$ and received vector $\mathbf{u}[i]$ is

$$\begin{aligned} \mathbf{u}[i] &= \underbrace{\mathbf{W}\mathbf{F}_1\mathbf{H}_0\mathbf{F}_0\mathbf{W}^\dagger}_{\mathbf{A}}\mathbf{s}[i] + \underbrace{\mathbf{W}\mathbf{F}_1\mathbf{H}_1\mathbf{F}_0\mathbf{W}^\dagger}_{\mathbf{B}}\mathbf{s}[i-1] + \underbrace{\mathbf{W}\mathbf{F}_1\mathbf{H}_2\mathbf{F}_0\mathbf{W}^\dagger}_{\mathbf{C}}\mathbf{s}[i+1] + \underbrace{\mathbf{W}\mathbf{F}_1\mathbf{n}[i]}_{\mathbf{e}[i]} \\ &= \mathbf{A}\mathbf{s}[i] + \mathbf{B}\mathbf{s}[i-1] + \mathbf{C}\mathbf{s}[i+1] + \mathbf{e}[i]. \end{aligned} \quad (3.15)$$

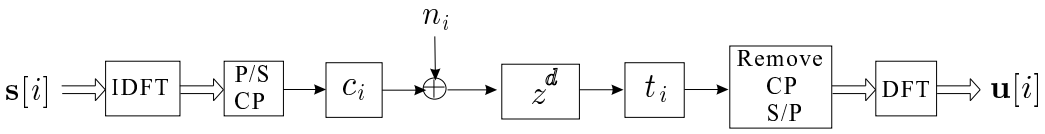

Figure 3.6: The block diagram of a DMT system with TEQ.

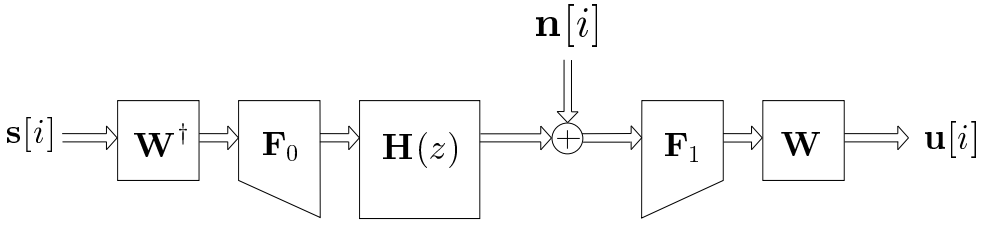

Figure 3.7: Matrix representation of DMT system and TEQ.

3.2 Output PSD of a DMT Transmitter

The DMT transmitter can be implemented as Figure 3.8.(a). Let us define the matrix $\mathbf{G}$ as

$$\mathbf{G} = \mathbf{F}_0 \mathbf{W}^\dagger. \tag{3.16}$$

As $\mathbf{G}$ is a constant matrix, we can exchange $\mathbf{G}$ and the expanders and redraw Figure 3.8.(b) in 3.8.(c). The M-input-one-output system from $\mathbf{p}[i]$ to g_i is LTI. Let's call the $M \times 1$ system $\mathbf{f}(z)$ with

$$\mathbf{f}(z) = [\, F_0(z) \quad F_1(z) \quad \cdots \quad F_{M-1}(z) \,]. \tag{3.17}$$

Then

$$\mathbf{f}(z) = [\, 1 \quad z^{-1} \quad \cdots \quad z^{-(N-1)} \,]\, \mathbf{G}. \tag{3.18}$$

The k-th transmitting filter $f_k[i]$ is defined by $F_k(z) = \sum_{i=0}^{N-1} z^{-i} G_{ik}$, with impulse response

$$f_k[i] = \frac{1}{\sqrt{M}} e^{-j\frac{(i-L)k}{M}}, \quad i = 0, 1, \cdots, N-1. \tag{3.19}$$

The DMT transmitter can be implemented by the filter bank defined above and shown in Figure 3.8.(d).

Assume the input $s_k[i]$ of the expander is a WSS process and zero-mean. The mean and autocorrelation of the output of expander $v[i]$ are

$$\begin{aligned} E[v[i]] &= 0, \\ R_v[n,m] &= E[v[n]v^*[m]] \\ &= \begin{cases} E[s_k[\lfloor \frac{n}{N} \rfloor] s_k^*[\lfloor \frac{m}{N} \rfloor]], & n/N \text{ and } m/N \text{ are integers.} \\ 0, & \text{otherwise.} \end{cases} \end{aligned} \tag{3.20}$$

where $\lfloor x \rfloor$ denotes the largest integer smaller or equal to x. From Equation 3.20, we can conclude that the output of the expader is a WCSS process with period N if the input is a WSS process. And the average PSD of the WCSS process $p_k[i]$ is

$$\overline{S}_{p_k}(e^{j\omega}) = \frac{1}{N} S_{s_k}(e^{j\omega}). \tag{3.21}$$

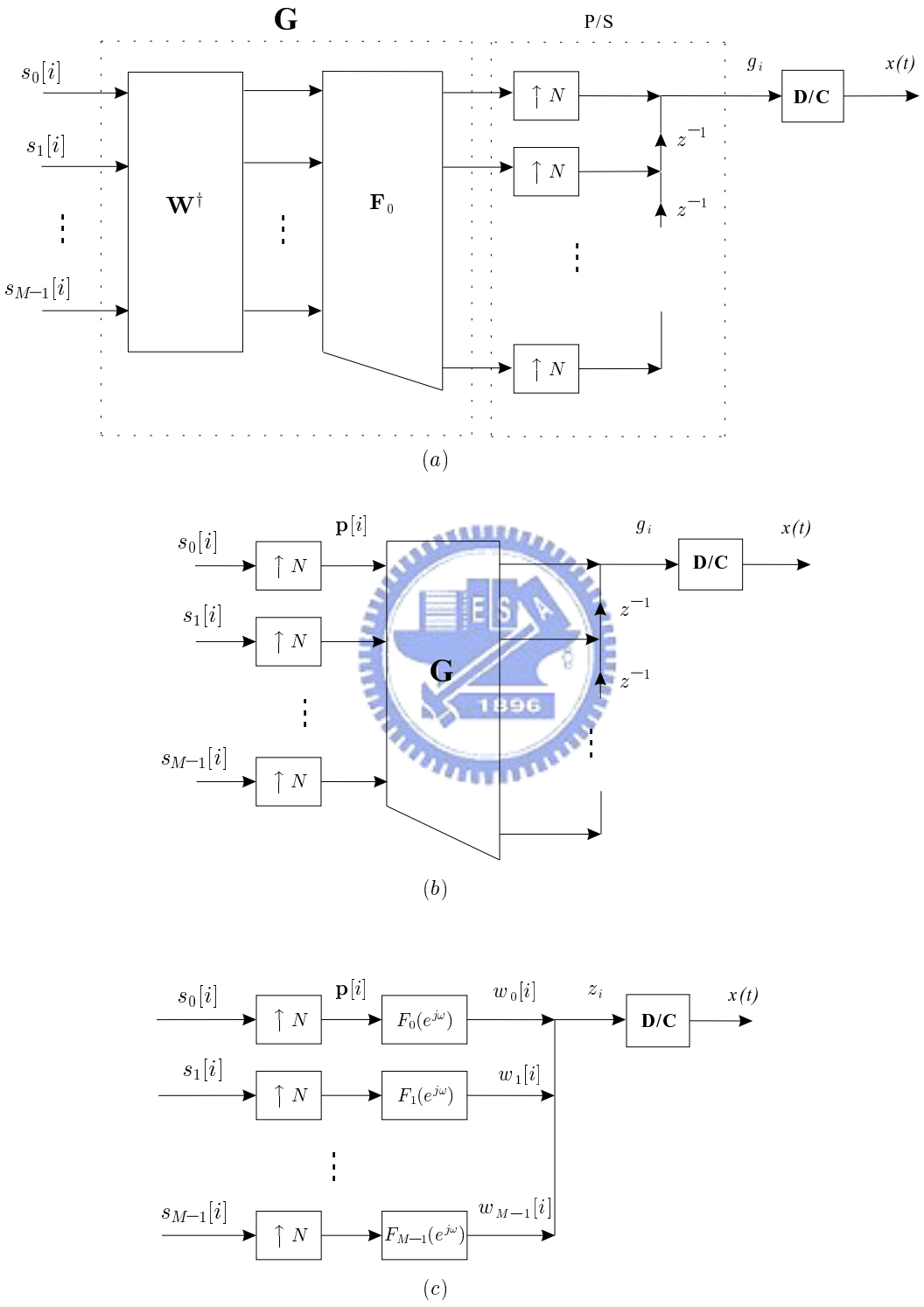

Figure 3.8: DMT transmitter.

As the input of the transmitter filter $F_k(e^{j\omega})$ is a WCSS process, the output $w_k[i]$ in Figure 3.8.(d) is also a WCSS process and the average PSD of $w_k[i]$ can be obtained,

$$\overline{S}_{w_k}(e^{j\omega}) = \frac{S_{s_k}(e^{j\omega})}{N}|F_k(e^{j\omega})|^2. \tag{3.22}$$

In DMT system, the inputs are in conjugate pairs, $s_k[i] = s^*_{M-k}[i]$. Let us expressed $s_k[i]$ in terms of real part $a_k[i]$ and imaginary part $b_k[i]$ as

$$s_k[i] = a_k[i] + jb_k[i]. \tag{3.23}$$

And assume $a_k[i]$ and $b_k[i]$ are uncorrelated, joint WSS with autocorrelation functions $R_{a_k}[i] = R_{b_k}[i] = \delta[i]\epsilon_{s_k}/2$, where the scalar $1/2$ is included so the $e[|s_k[i]|^2] = \epsilon_{s_k}$. Notice that the k-th and the $(M-k)$-th transmitting filters are also in complex conjugate pairs, $f_k[i] = f^*_{M-k}[i]$. Express $f_k[i]$ in terms of real part $f_{k,real}[i]$ and imaginary part $f_{k,imag}[i]$ as

$$f_k[i] = f_{k,real}[i] + jf_{k,imag}[i]. \tag{3.24}$$

The the output of the transmitting filter $w_k[i]$ and $w_{M-k}[i]$ in Figure 3.8.(d) are complex conjugate of each other. Define

$$w'_k[i] = w_k[i] + w_{M-k}[i], \tag{3.25}$$

then $w'_k = 2Real\{w_k[i]\}$ and it can be written as

$$w'_k[i] = 2\sum_l (a_k[l]f_{k,real}[i-Nl] - b_k[l]f_{k,imag}[i-Nl]) \tag{3.26}$$

as the $a_k[i]$ and $b_k[i]$ are uncorrelated, we can obtain the average PSD of w'_k,

$$\overline{S}_{w_{k'}}(e^{j\omega}) = \frac{2\epsilon_{s_k}}{N}(|F_{k,real}(e^{j\omega})|^2 + |F_{k,imag}(e^{j\omega})|^2), \tag{3.27}$$

where $F_{k,real}(e^{j\omega})$ and $F_{k,imag}(e^{j\omega})$ are respectively the Fourier transform of $f_{k,real}[i]$ and $f_{k,imag}[i]$. On the other hand, notice that $F_k(e^{j\omega}) = F_{k,real}(e^{j\omega}) + jF_{k,imag}(e^{j\omega})$. With $f_{M-k}[i] = f_{k,real}[i] - jf_{k,imag}[i]$, we have $F_{M-k}(e^{j\omega}) = F_{k,real}(e^{j\omega}) - jF_{k,imag}(e^{j\omega})$. We can verify that,

$$|F_k(e^{j\omega})|^2 + |F_{M-k}(e^{j\omega})|^2 = 2(|F_{k,real}(e^{j\omega})|^2 + |F_{k,imag}(e^{j\omega})|^2). \tag{3.28}$$

As a result

$$\overline{S}_{w'_k}(e^{j\omega}) = \frac{\epsilon_{s_k}}{N}(|F_k(e^{j\omega})|^2 + |F_{M-k}(e^{j\omega})|^2). \tag{3.29}$$

The transmitted average PSD $S_g(e^{j\omega})$ is the summation of$\overline{S}_{w'_k}(e^{j\omega})$, plus $S_0(e^{j\omega})$ and $S_{M/2}(e^{j\omega})$ if M is even. Therefore, we have

$$\overline{S}_g(e^{j\omega}) = \frac{1}{N}\sum_{k=0}^{M-1}\epsilon_{s_k}|F_k(e^{j\omega})|^2, \tag{3.30}$$

As a result, the output signal $x(t)$ of the D/C converter becomes a WCSS process with period NT as g_i is a WCSS process with period N. The PSD of $x(t)$ is

$$\overline{S}_x(j\Omega) = \frac{1}{NT}\sum_{k=0}^{M-1}\epsilon_{s_k}|F_k(e^{j\Omega T})|^2|H_r(j\Omega)|^2 \tag{3.31}$$

3.3 Transmitter PSD for DSL System

In DSL system, FDD is used to separate the upstream and downstream data. For example, Figure 3.9 shows the PSD for upstream and downstream transmission of Very high speed Digital Subscriber Line (VDSL) system. Then, the tone indexes for upstream and downstream are listed in Table 3.1. The tones with indexes $5, 6\cdots32$ are reserved for optional upstream transmission.

Table 3.1: Tone index of upstream and downstream band.

Upstream	$5, 6\cdots32, 871, 872\cdots1205, 1972, 1973\cdots2783$
Downstream	$33, 34\cdots870, 1206, 1207\cdots1971$

In downstream transmission, the upstream tones are not used and are referred to the null tones. Similarity, the upstream transmission the downstream tones are used the null tones. In VDSL system, $M = 8192$, $L = 640$ and $\frac{1}{T} = 35.328MHz$. $F_0(e^{j\Omega T})$ is a narrow band filter, we show the The magnitude response of $F_0(e^{j\omega})$ in Figure 3.10. The samples of $\overline{S}_x(j\Omega)$ can be written as

$$\overline{S}_x(\jmath\Omega)|_{\Omega=\frac{2\pi k}{MT}} \simeq \frac{1}{NT}\epsilon_{s_k}|F_k(e^{j\frac{2\pi k}{M}})|^2|H_r(j\frac{2\pi k}{MT})|^2. \tag{3.32}$$

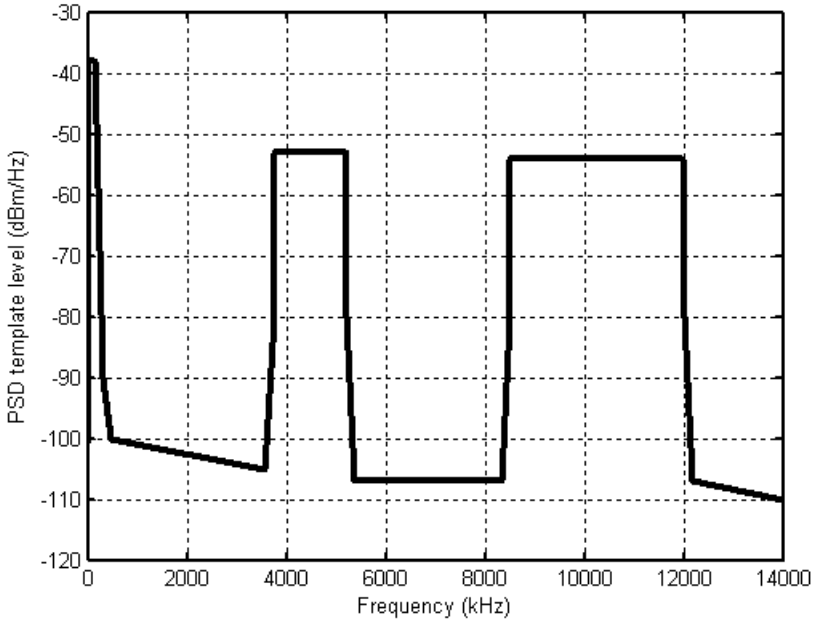

(a)

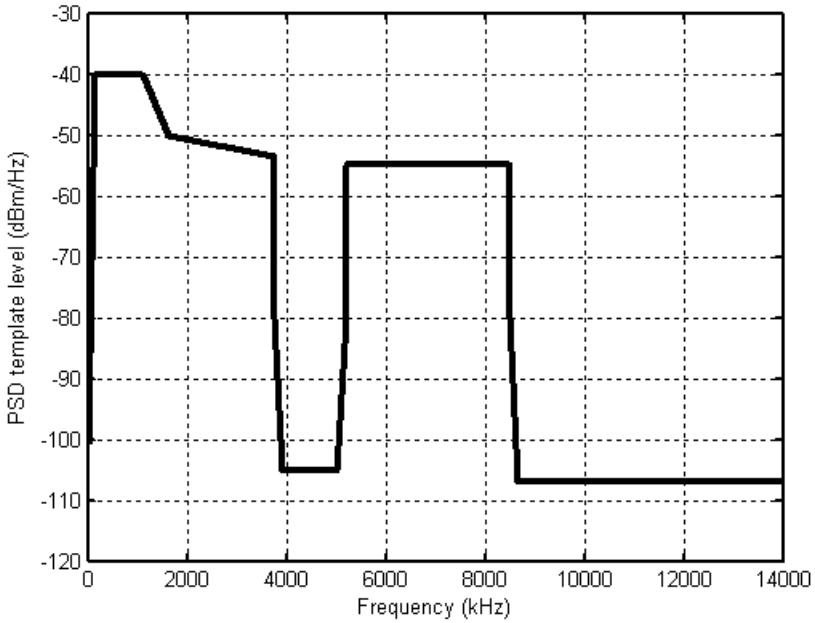

(b)

Figure 3.9: PSD template, (a) upstream, (b) downstream.

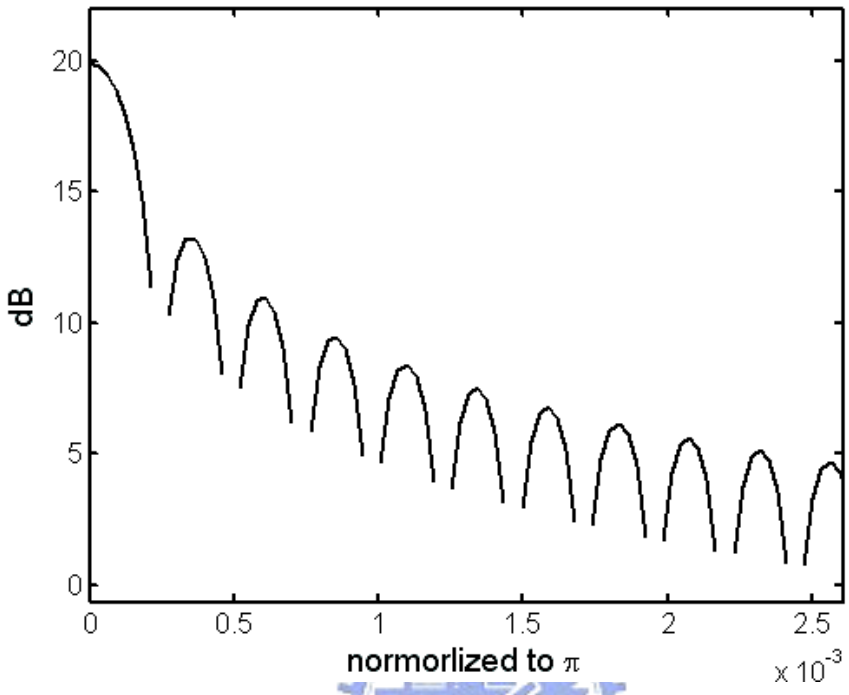

Figure 3.10: Magnitude response of $F_0(e^{j\omega})$.

We have $|F_k(e^{j\frac{2\pi k}{M}})| = |F_0(e^{j0})| = \frac{N}{\sqrt{M}}$ and assume the reconstruction filter $|H_r(j\Omega)|^2 = T^2,\ |\Omega| < \frac{1}{2T}$. Equation 3.32 can be expressed as

$$\begin{aligned} \overline{S}_x(\jmath\Omega)|_{\Omega=\frac{2\pi k}{MT}} &\simeq \frac{1}{NT}\epsilon_{s_k} \cdot \frac{N^2}{M} \cdot T^2 \\ &= \frac{\epsilon_{s_k} NT}{M}. \end{aligned} \tag{3.33}$$

Assume the amplitude of the transmitter PSD is $-60dBm/Hz = -90dBW/Hz$ in the used bands, and the signal power is measured across a terminated resistor $R_v = 100Ohm$. The k-th tone belongs to used tones signal power can be obtained using Equation 3.33,

$$\epsilon_{s_k} \simeq \frac{M\overline{S}_x(\jmath\Omega)}{NT}|_{\Omega=\frac{2\pi k}{MT}} \quad (V^2), \tag{3.34}$$

with

$$\overline{S}(j\frac{2\pi k}{MT}) \simeq 10^{-9} \cdot R_v = 10^{-7} \quad (V^2).$$

We can calculate the signal power as following,

$$\begin{aligned} \epsilon_{s_k} &\simeq \frac{10^{-9}M}{NT} \quad (Watt) \\ &= \frac{10^{-9} \cdot R_v M}{NT} = \frac{10^{-7}M}{NT} \quad (V^2). \end{aligned} \tag{3.35}$$

Therefore the output PSD of the transmitter is shown in Figure 3.11.

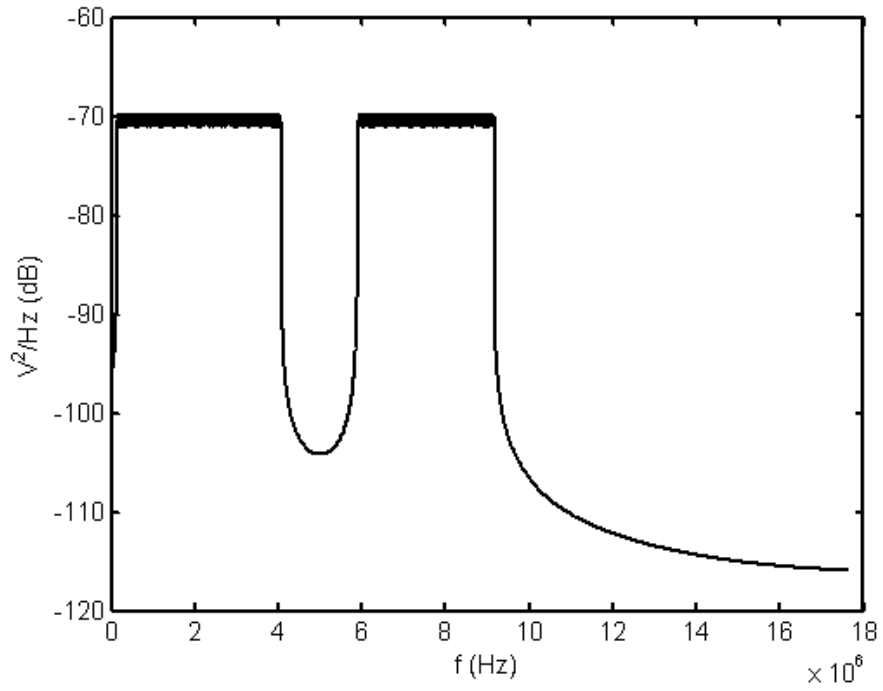

Figure 3.11: PSD example: VDSL downstream transmission.

3.4 Generation of Noise for VDSL System

In this section, we will give two noise generating examples, one is white noise and other one is Far-End crosstalk (FEXT) noise in VDSL system [2]. The Near-End crosstalk (NEXT) noise can be generated using the same step as FEXT noise. In VDSL system, T is $\frac{1}{(35.328\times10^6)}$, block size M is 8192, and CP length L is 640.

3.4.1 White Noise

For example, The continuous white noise PSD is $-170dBm/Hz$ in VDSL system and it is measured across a terminated resistor $R_v = 100Ohm$. The continuous white noise PSD is

$$S_{e_c}(j\Omega) = 10^{-170/10} \cdot 10^{-3} \cdot R_v = 10^{-18} \quad (V^2). \tag{3.36}$$

Assume the magnitude response of antialiasing filter before the C/D converter $|H_a(j\Omega)|^2 = 1 \forall |\Omega| < \frac{\pi}{T}$. The discrete white noise PSD is

$$S_e(e^{j\omega}) = 10^{-18} \cdot 35328000 \cdot 1 = -104.5 \quad (dB).$$

The continuous white noise PSD, frequency response and discrete white noise are shown in Figure 3.12.

3.4.2 FEXT Noise

The FEXT noise PSD in VDSL system can be obtained in [2]. The FEXT noise generator is shown in Figure 3.13, in which $g(t)$ is generated as the alian cross talk noise. The PSD of $g(t)$ is

$$S_g(j\Omega) = \overline{S}_x(j\Omega) \cdot 10^{0.8} \quad (V^2), \tag{3.37}$$

and it is measured across a terminated resistor $R_v = 100Ohm$. The PSD $S_g(j\Omega)$ is the PSD $S_{x_c}(j\Omega)$ adding 8dB, the addition of 8dB approximates the power generated by the sum of 20 VDSL systems operating in a multi-pair cable. The magnitude square of the crosstalk transfer function $H_2(j\Omega, L)$ is

$$|H_2(j\Omega, L)|^2 = |H(j\Omega)|^2 \cdot K_{fext} \cdot (1/49)^{0.6} \cdot L \cdot (\Omega/2\pi)^2, \tag{3.38}$$

where $H(j\Omega)$ is channel frequency response, the coefficient $K_{fext} = 2.44 \times 10^{-22}$ and $L(feet)$ is the length of twisted pair loop. From Equation 2.16, the PSD of discrete FEXT noise $e[n]$ is

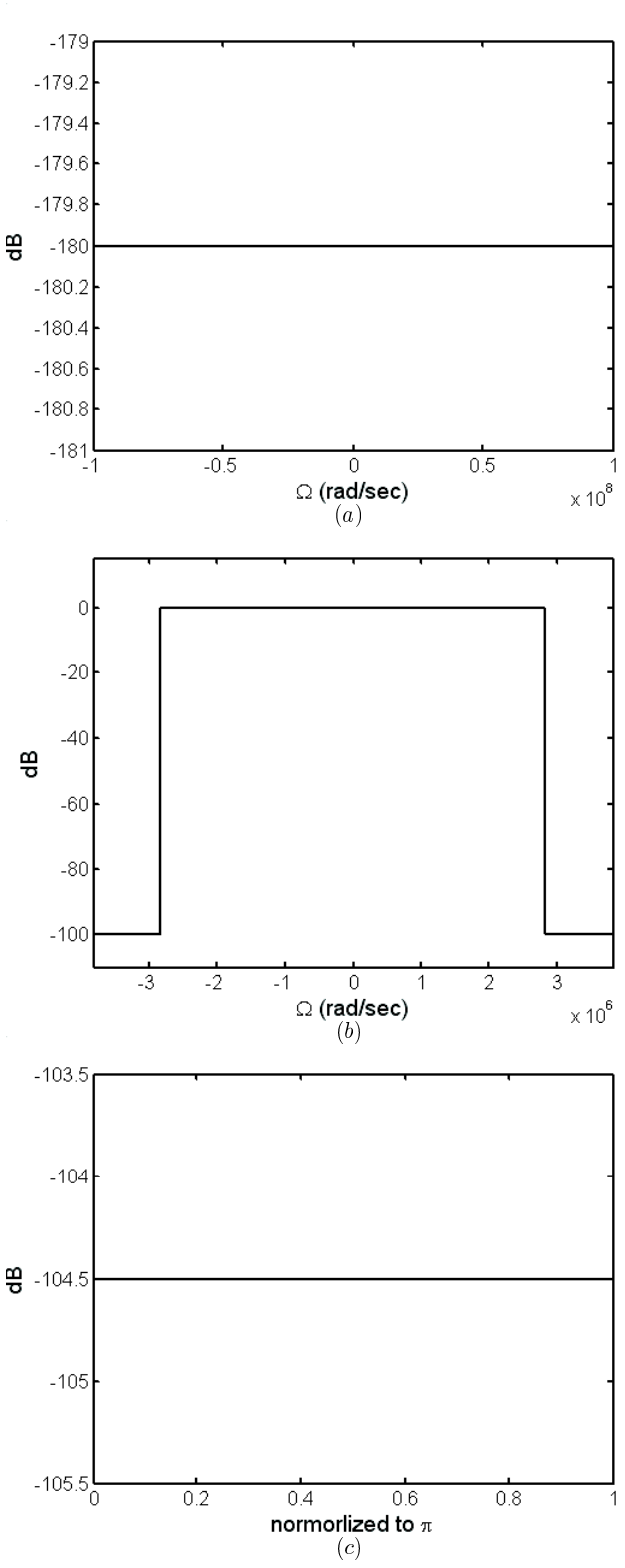

Figure 3.12: (a) Continuous white noise PSD $S_{e_c}(jf)$. (b) Frequency response of antialiasing filter. (c) Discrete white noise PSD $S_e(e^{j\omega})$.

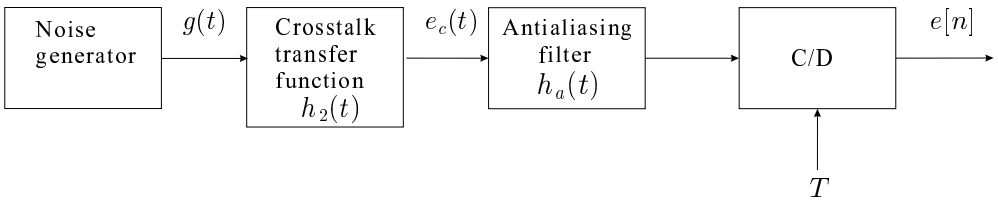

Figure 3.13: FEXT noise generator.

$$S_e(e^{j\omega}) = \frac{1}{T} S_{e_c}(j\frac{\omega}{T}), \quad |\omega| \leq \pi, \tag{3.39}$$

as the $h_a(t) = \frac{sin\frac{\pi t}{T}}{\pi t}$. To generate a random sequence with PSD $S_e(e^{j\omega})$, we can pass a white sequence through a FIR filter $h_f[n]$. The FIR filter is obtained from 32768-point IDFT of the 32768 samples of $S_e(e^{j\omega})$ over $\omega = \{0 \sim 2\pi\}$. To shorten the length of $h_f[n]$, we will add a length 257 Hanning window on the impulse response of 8192-point IDFT of the 8192 samples of $S_e(e^{j\omega})$, i.e.,

$$h_f[n] \;\; = \;\; h_{han}[n] \cdot IDFT\{S_e(e^{j\frac{2\pi k}{32768}})\}, \tag{3.40}$$

where $S_e(e^{j\frac{2\pi k}{32768}})$ are the 32768 samples of $S(e^{j\omega})$ over $\omega = \{0 \sim 2\pi\}$. With

$$h_{han}[n] = \begin{cases} 0.5 - 0.5 \cdot cos(2\pi n/257), & 0 \leq n \leq 257 \\ 0, & otherwise \end{cases}. \tag{3.41}$$

Figure 3.14.(a) shows the PSD of $S_g(j\Omega)$, 3.14.(b) shows the magnitude response of channel $|H(j\Omega)|^2$, 3.14.(c) shows the magnitude response of $h_2(t)$ filter $|H_2(j\Omega, L)|^2$, 3.14.(d) shows the PSD of continuous time FEXT noise $S_{e_c}(j\Omega)$, 3.14.(e) shows the PSD of discrete time FEXT noise $S_e(j\Omega)$ and 3.14.(f) shows the FEXT noise generated by a white noise sequence passing through the filter $h_f[n]$.

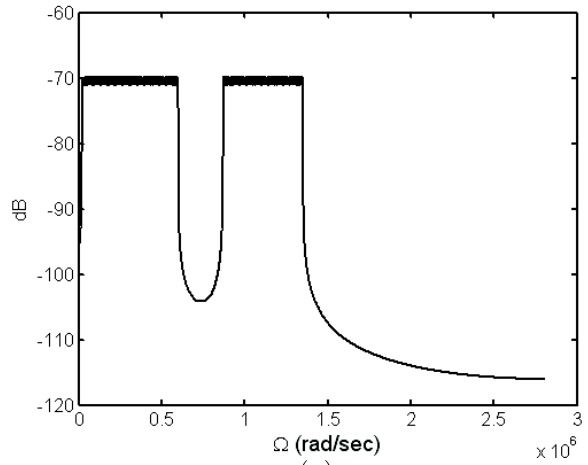
-60
-70
-80
-90
-100
-110
-120
dB
0
0.5
1
1.5
2
2.5
3
Ω (rad/sec)
x 10^6

(a)

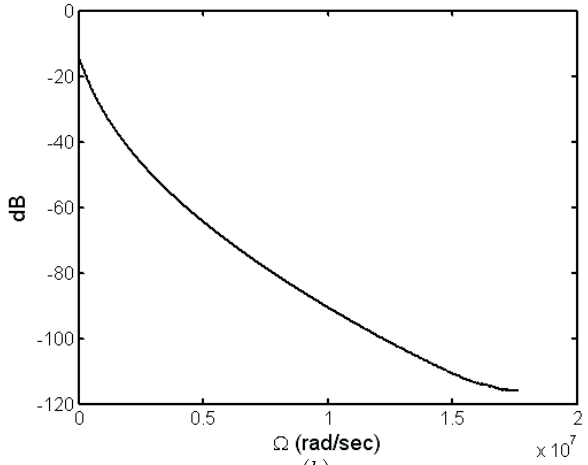
0
-20
-40
-60
-80
-100
-120
dB
0
0.5
1
1.5
2
Ω (rad/sec)
x 10^7

(b)

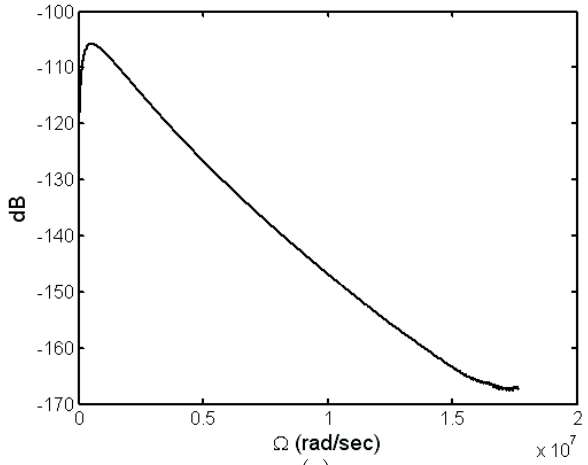
-100
-110
-120
-130
-140
-150
-160
-170
dB
0
0.5
1
1.5
2
Ω (rad/sec)
x 10^7

(c)

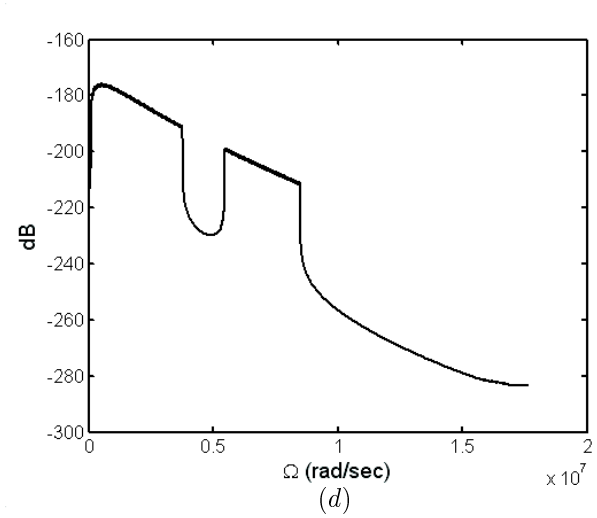

(d)

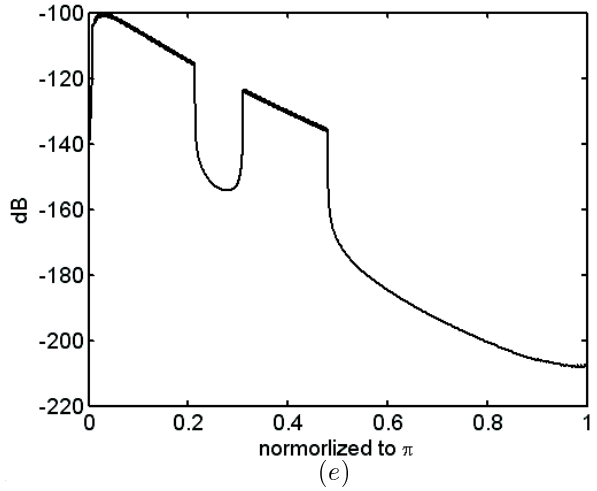

(e)

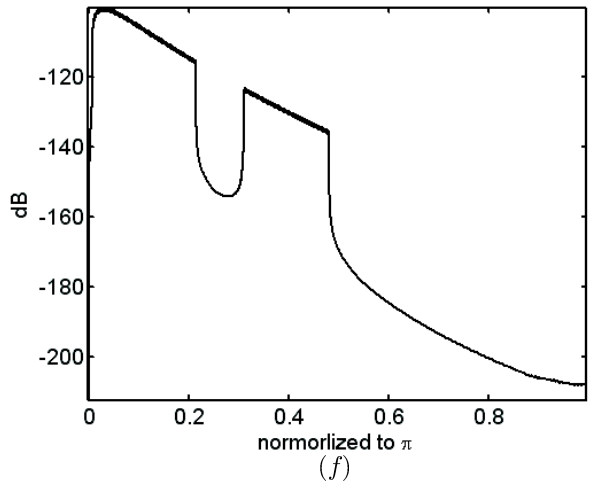

(f)

Figure 3.14: (a) The PSD of $S_g(j\Omega)$, (b) the magnitude response of channel $|H(j\Omega)|^2$, (c) the magnitude response of $h_2(t)$, (d) the PSD of continuous time FEXT noise $S_{e_c}(j\Omega)$ (e) the PSD of discrete time FEXT noise $S_e(j\Omega)$ (f) the PSD of FEXT noise generated by a white noise sequence passing through the filter $h_f[n]$.

Chapter 4

Previous TEQ Designs

This chapter is a survey of 2 TEQ designs that we will compare with our proposed TEQ.

4.1 MSSNR Algorithm

In DMT system, we have known that the channel can be considered as M parallel sub-channels if the channel order is smaller than L. If channel order is larger than L, ISI raised. We can shorten the channel into a length $L+1$ window with starter point d, then, the ISI power be eliminated. To measure the channel shorten effect, we can define the SIR, it is the energy inside the length $L+1$ window over the energy outside the length $L+1$ window.

$$\text{SIR} = \max_{d} \frac{\sum_{i=d}^{d+L} h_i^2}{\sum_{i=0, i\neq(d,\cdots d+L)}^{\nu} h_i^2}. \tag{4.1}$$

In [3], a maximal SIR TEQ be proposed, it derived the SIR as a quadratic form and solve the optimal solution by Rayleigh principle.

The equalized channel coefficient, $h_i = c_i * t_i$, can be represented as two matrix multiplying, and $\mathbf{t}$ is a $T_e \times 1$ vector represents TEQ coefficient.

$$\mathbf{h}_{equ} = \begin{bmatrix} h_0 \\ h_1 \\ \vdots \\ h_{\nu+T_e-1} \end{bmatrix}$$

$$= \begin{bmatrix} c_0 & 0 & \cdots & \cdots & 0 \\ c_1 & c_0 & \ddots & & \vdots \\ \vdots & \ddots & & & \vdots \\ c_\nu & c_{\nu-1} & \cdots & c_{\nu-T_e+2} & c_{\nu-T_e+1} \\ 0 & c_\nu & \cdots & & c_{\nu-T_e+2} \\ \vdots & \ddots & & & \vdots \\ 0 & \cdots & & 0 & c_\nu \end{bmatrix} \begin{bmatrix} t_0 \\ t_1 \\ \vdots \\ t_{T_e-1} \end{bmatrix}. \tag{4.2}$$

The coefficients inside and outside the window can be expressed as h_{win} and h_{wall}.

$$\begin{aligned} \mathbf{h}_{win} &= \begin{bmatrix} h_d \\ h_{d+1} \\ \vdots \\ h_{d+L} \end{bmatrix} \\ &= \begin{bmatrix} c_d & c_{d+1} & \cdots & c_{d+T_e-1} \\ c_{d+1} & c_d & \cdots & \vdots \\ \vdots & & \ddots & \vdots \\ c_{d+L} & c_{d+L-1} & \cdots & c_{d+L-T_e+1} \end{bmatrix} \begin{bmatrix} t_0 \\ t_1 \\ \vdots \\ t_{T_e-1} \end{bmatrix} \\ &= \mathbf{C}_{win}\mathbf{t}, \end{aligned} \tag{4.3}$$

$$\begin{aligned} \mathbf{h}_{wall} &= \begin{bmatrix} h_0 \\ \vdots \\ h_{d-1} \\ h_{d+L+1} \\ \vdots \\ h_{\nu+T_e-1} \end{bmatrix} \\ &= \begin{bmatrix} c_0 & 0 & \cdots & 0 \\ \vdots & \ddots & & \\ c_{d-1} & c_{d-2} & \cdots & c_{d-T_e} \\ c_{d+L+1} & c_{d+L} & \cdots & c_{d+L-T_e+2} \\ \cdots & \ddots & & \\ 0 & \cdots & 0 & c_\nu \end{bmatrix} \begin{bmatrix} t_0 \\ t_1 \\ \vdots \\ t_{T_e-1} \end{bmatrix} \\ &= \mathbf{C}_{wall}\mathbf{t}. \end{aligned} \tag{4.4}$$

The SIR defined in Equation 4.1 can be expressed as

$$\text{SIR} = \frac{\mathbf{h}_{win}^\dagger \mathbf{h}_{win}}{\mathbf{h}_{wall}^\dagger \mathbf{h}_{wall}} = \frac{\mathbf{t}^\dagger \mathbf{C}_{win}^\dagger \mathbf{C}_{win}\mathbf{t}}{\mathbf{t}^\dagger \mathbf{C}_{wall}^\dagger \mathbf{C}_{wall}\mathbf{t}}. \tag{4.5}$$

The optimal TEQ shall be chosen to maximize $\mathbf{h}_{win}^\dagger \mathbf{h}_{win}$ while $\mathbf{h}_{wall}^\dagger \mathbf{h}_{wall} = 1$. The matrix $\mathbf{C}_{wall}^\dagger \mathbf{C}_{wall}$ is Hermitian and positive semidefinite typically, however, we

can assume it be a positive definite matrix. Because the eigenvalue of $\mathbf{C}_{wall}^{\dagger}\mathbf{C}_{wall}$ equals zero means there exists ISI free TEQ but it is rare the case. If $\mathbf{C}_{wall}^{\dagger}\mathbf{C}_{wall}$ is positive definite, we can perform Cholesky decomposition on it, $\mathbf{C}_{wall}^{\dagger}\mathbf{C}_{wall} = \mathbf{R}^{\dagger}\mathbf{R}$ and $\mathbf{R}^{\dagger} = \mathbf{R}^{-1}$, since $\mathbf{C}_{wall}^{\dagger}\mathbf{C}_{wall}$ is full rank, $\mathbf{R}$ is invertible. Then,

$$\mathbf{t}^{\dagger}\mathbf{C}_{wall}^{\dagger}\mathbf{C}_{wall}\mathbf{t} = \mathbf{t}^{\dagger}\mathbf{R}^{\dagger}\mathbf{R}\mathbf{t}. \tag{4.6}$$

For finding the solution of cost function, let $\mathbf{v} = \mathbf{R}\mathbf{t}$, the optimization problem now is

$$\underset{\mathbf{v}}{max} \quad \frac{\mathbf{v}^{\dagger}\mathbf{R}\mathbf{C}_{win}^{\dagger}\mathbf{C}_{win}\mathbf{R}^{-1}\mathbf{v}}{\mathbf{v}^{\dagger}\mathbf{v}}. \tag{4.7}$$

According to Rayleigh principle, the solution $\mathbf{v}$ is the eigenvector corresponding to the maximal eigenvalue of $(\mathbf{R}^{-1})^{\dagger}\mathbf{C}_{win}^{\dagger}\mathbf{C}_{win}\mathbf{R}^{-1}$ and SIR equals the maximal eigenvalue. Solving

$$\mathbf{t} = \mathbf{R}^{-1}\mathbf{v}, \tag{4.8}$$

the optimal TEQ $\mathbf{t}$ obtained. The TEQ is dependent on delay d, we should exhaustive search the optimal TEQ as the maximal SIR on possible delay appears. MSSNR provides a solution for maximal SIR, it is appropriate for TEQ performance comparison. In Figure 4.1, the impulse responses of VDSL loop 7 and the equalized channel using MSSNR algorithm are shown, we can see that the channel be shortened. The SIR of the original and equalized channels are $35.79dB$ and $76.06dB$.

4.2 MERRY Algorithm

After CP block, the first L transmitted samples is repeating the last L samples. Convolving the channel, the relationship be destroyed because ISI raised. For example,

$L = 2, \nu = 3$ and $M = 8$,

$r_1 = c_0 \cdot x_1 + c_1 \cdot x_0 + c_2 \cdot x_{-1} + c_3 \cdot x_{-2}$,

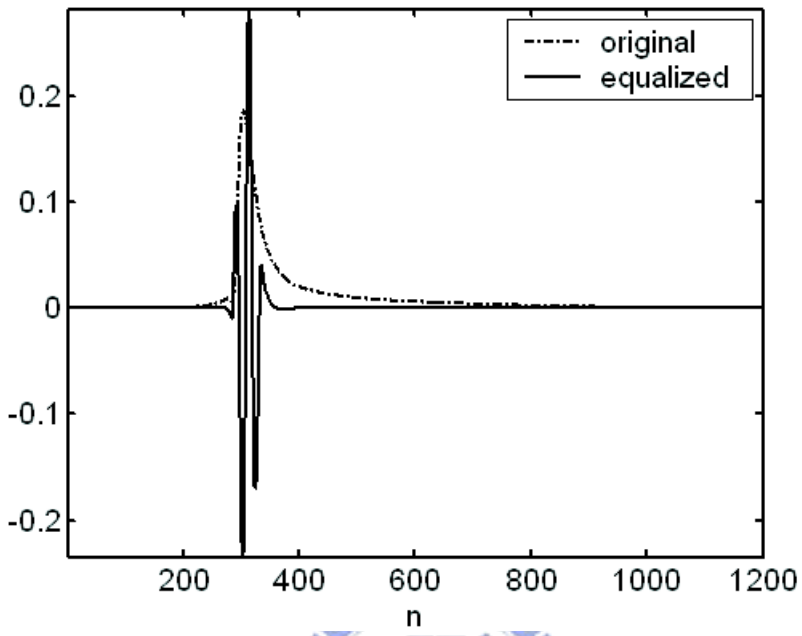

Figure 4.1: MSSNR: VDSL loop 7, $L = 640$, $d = 7$.

$$r_9 = c_0 \cdot x_9 + c_1 \cdot x_8 + c_2 \cdot x_7 + c_3 \cdot x_6 = c_0 \cdot x_1 + c_1 \cdot x_0 + c_2 \cdot x_7 + c_3 \cdot x_6,$$

where r_i is the received sequence before TEQ block. If c_2 and c_3 equal zero, $r_1 = r_9$. MERRY [4], a blind and adaptive TEQ algorithm, is trying to force c_2 and c_3 to be zero, then, shorten the channel. The cost function of MERRY can be expressed as

$$J_d = E[|y_d - y_{M+d}|^2], \ d \in (0, \cdots \nu) \tag{4.9}$$

where d is the optimal delay and same with synchronization delay and $y_i = r_i * t_i$. Based on the concept, we can modified the cost function for fast convergence.

$$J_{d,mod} = \sum_i E[|y_{d+i} - y_{M+d+i}|^2], \tag{4.10}$$

where i can be chosen as a continuous sequence and $d + i \in (0, \cdots \nu)$. To solve Equation 4.10, we can perform a stochastic gradient descent method. Getting the instant cost function

$$J_{d,inst} = \sum_i |y_{d+i} - y_{M+d+i}|^2, \tag{4.11}$$

and the gradient

$$\frac{\partial J_{d,inst}}{\partial t_l} = \sum_i (y_{d+i} - y_{M+d+i})(r_{d+i-l} - r_{M+d+i-l}). \tag{4.12}$$

Define

$$\begin{aligned} \tilde{e}_i &= (y_{d+i} - y_{M+d+i}) \\ \tilde{d}_i &= (r_{d+i-l} - r_{M+d+i-l}). \end{aligned} \tag{4.13}$$

TEQ can be obtained by updating

$$\begin{aligned} t^{k+1}(l) &= t^k(l) - \mu \frac{\partial J_{d,inst}}{\partial t(l)} \\ &= t^k(l) - \mu \sum_i \tilde{e}_i \cdot \tilde{d}_i. \end{aligned} \tag{4.14}$$

For avoiding trivial solution $\mathbf{t} = [0, \cdots 0]^\dagger$, the TEQ should be normalized as

$$\mathbf{t}^{k+1} = \frac{\mathbf{t}^{k+1}}{(\mathbf{t}^{k+1})^\dagger \mathbf{t}^{k+1}}. \tag{4.15}$$

In the gradient descent method, the optimal delay should be given first, we prefer setting the start point of the maximal SIR of original channel c_i as the optimal delay. In Figure 4.2, the impulse responses of VDSL loop 7 and the equalized channel using MERRY algorithm are shown, we can see that the channel be shortened. The SIR of the original and equalized channels are $35.79dB$ and $44.78dB$.

4.3 MFSIR Algorithm

In training pahse of VDSL system, the pilot tones are assigned the same QAM symbol every DMT blocks. The elements of received output vector $\mathbf{u}[i]$ shown in Figure 3.6 will not be zero-mean. We can compute the mean of elements corresponding to pilot $\overline{\mathbf{d}}$ and null tones $\overline{\mathbf{n}}$,

$$\begin{aligned} \overline{\mathbf{d}} &= \frac{1}{N_a} \sum_{i=1}^{N_a} \mathbf{d}[i] \\ \overline{\mathbf{n}} &= \frac{1}{N_a} \sum_{i=1}^{N_a} \mathbf{n}[i], \end{aligned} \tag{4.16}$$

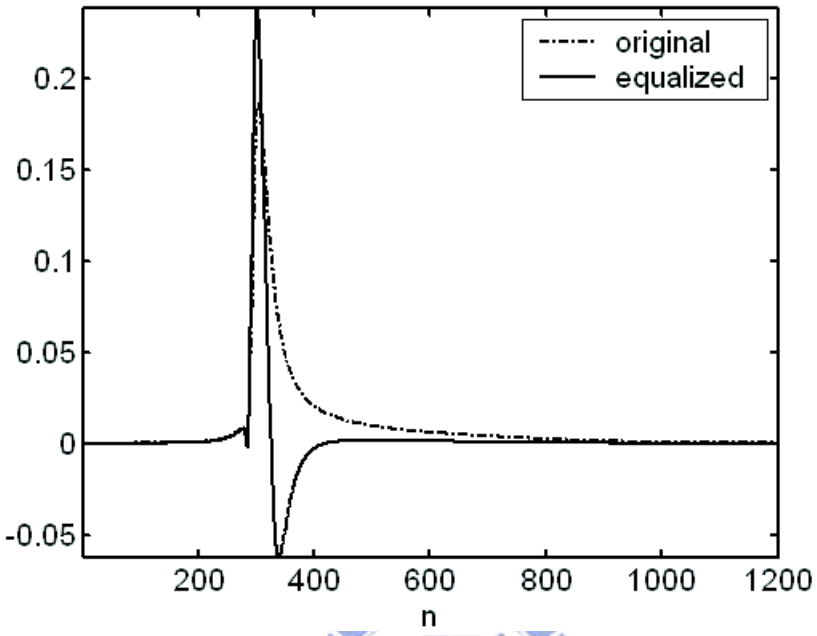

Figure 4.2: MERRY: VDSL loop 7, $L = 640$, $d = 227$.

where $\mathbf{d}[i]$ and $\mathbf{n}[i]$ are vectors whose elements are the elements of $\mathbf{u}[i]$ corresponding to pilot and null tones respectively, N_a is the number of collected block $\mathbf{u}[i]$. The averaged null tones elements $\overline{\mathbf{n}}$ is mostly the interference caused from pilot tones. The square of norm of $\overline{\mathbf{d}}$ and $\overline{\mathbf{n}}$ can be considered as power of pilot and null tone signals. We will maximize the ratio of pilot tone signals power over the null tone signals power and the cost function is

$$\phi = \frac{\overline{\mathbf{d}}^{\dagger}\overline{\mathbf{d}}}{\overline{\mathbf{n}}^{\dagger}\overline{\mathbf{n}}}.$$

From Figure 3.6 and the derivations of Section 3.1, the input vector of DFT block $\mathbf{y}[i]$ can be written in terms of the received sequence before TEQ r_i and TEQ coefficients t_i as

$$\mathbf{y}[i] = \underbrace{\begin{bmatrix} r_{iN+L+d} & r_{iN+L+d-1} & \cdots & r_{iN+L+d-T_e+1} \\ r_{iN+L+d+1} & r_{iN+L+d} & \cdots & r_{iN+L+d-T_e+2} \\ \vdots & \vdots & \ddots & \vdots \\ r_{(i+1)N+d-1} & r_{(i+1)N+d-2} & \cdots & r_{(i+1)N+d-T_e} \end{bmatrix}}_{\mathbf{R}_i} \underbrace{\begin{bmatrix} t_0 \\ t_1 \\ \vdots \\ t_{T_e-1} \end{bmatrix}}_{\mathbf{t}}, \qquad (4.17)$$

where $\mathbf{R_i}$ is a $M \times T_e$ matrix. The i-th pilot and null tone vectors $\mathbf{d}[i]$ and $\mathbf{n}[i]$ can be expressed as

$$\begin{aligned} \mathbf{d}[i] &= \mathbf{W}_1\mathbf{y}[i] \\ \mathbf{n}[i] &= \mathbf{W}_2\mathbf{y}[i], \end{aligned} \tag{4.18}$$

where $\mathbf{W}_1$ and $\mathbf{W}_2$ are the rows of $M \times M$ DFT matrix $\mathbf{W}$ corresponding to pilot and null tones respectively. Using Equation 4.17, we can write $\mathbf{d}[i]$ and $\mathbf{n}[\mathbf{i}]$ as

$$\mathbf{d}[\mathbf{i}] = \mathbf{W_1}\mathbf{R_i}\mathbf{t}, \quad \mathbf{n}[\mathbf{i}] = \mathbf{W_2}\mathbf{R_i}\mathbf{t}.$$

Then Equation 4.16 can be expressed as

$$\overline{\mathbf{d}}[i] = \mathbf{W}_1\overline{\mathbf{R}}\mathbf{t}, \quad \overline{\mathbf{n}}[\mathbf{i}] = \mathbf{W_2}\overline{\mathbf{R}}\mathbf{t},$$

where

$$\overline{\mathbf{R}} = \frac{1}{N_a}\sum_{i=1}^{N_a}\mathbf{R}_i.$$

Therefore we have

$$\begin{aligned} \overline{\mathbf{d}}^\dagger\overline{\mathbf{d}} &= \mathbf{t}^\dagger\underbrace{\overline{\mathbf{R}}^\dagger\mathbf{W}_1^\dagger\mathbf{W}_1\overline{\mathbf{R}}}_{\mathbf{A}}\mathbf{t} = \mathbf{t}^\dagger\mathbf{A}\mathbf{t} \\ \overline{\mathbf{n}}^\dagger\overline{\mathbf{n}} &= \mathbf{t}^\dagger\underbrace{\overline{\mathbf{R}}^\dagger\mathbf{W}_2^\dagger\mathbf{W}_2\overline{\mathbf{R}}}_{\mathbf{B}}\mathbf{t} = \mathbf{t}^\dagger\mathbf{B}\mathbf{t}. \end{aligned} \tag{4.19}$$

The cost function can be expressed as

$$\phi = \frac{\mathbf{t}^\dagger\mathbf{A}\mathbf{t}}{\mathbf{t}^\dagger\mathbf{B}\mathbf{t}}.$$

The optimal problem can be rewritten as

$$\begin{aligned} &\max_{\mathbf{t}} \ \mathbf{t}^\dagger\mathbf{A}\mathbf{t} \qquad ll) \\ &\text{subject to } \mathbf{t}^\dagger\mathbf{B}\mathbf{t} = \mathbf{1} \end{aligned} \tag{4.20}$$

Solving Equation **??** leads to a TEQ that satisfies the eigen problem

$$\mathbf{A}\mathbf{t} = \lambda\mathbf{B}\mathbf{t}.$$

The optimal solution $\mathbf{t}$ is the eigenvector corresponding to the largest eigenvalue of $\mathbf{B}^{-1}\mathbf{A}$. In Figure 4.3, the impulse responses of VDSL loop 7 and the equalized channel using MFSIR algorithm are shown, we can see that the channel be shortened. The SIR of the original and equalized channels are $35.79dB$ and $58.28dB$.

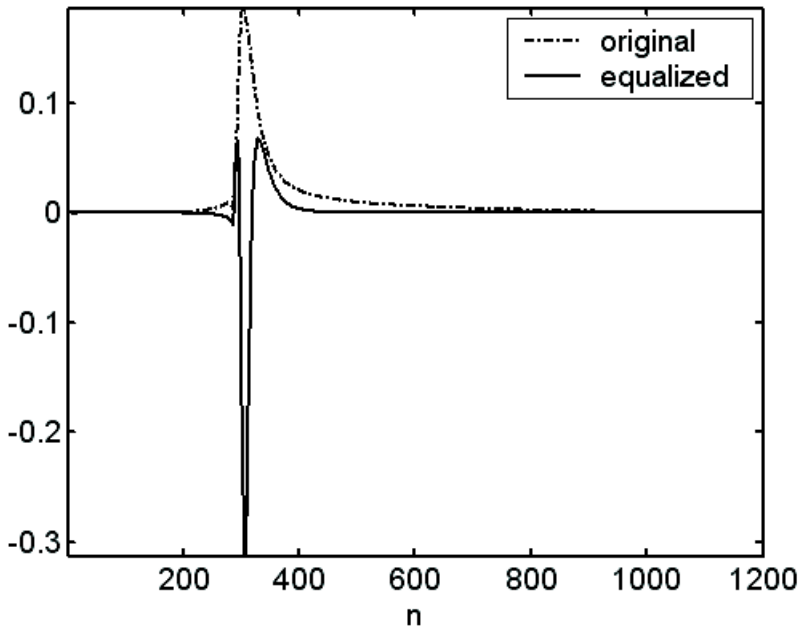

Figure 4.3: MFSIR: VDSL loop 7, $L = 640$, $d = 0$.

Chapter 5

Proposed TEQ Design

In Section 3.2, we derived the relation between the receiver output vector and the transmitter input vector. We repeat it here for convenience.

$$\mathbf{u}[i] \;=\; \mathbf{A}\mathbf{s}[i] + \mathbf{B}\mathbf{s}[i-1] + \mathbf{C}\mathbf{s}[i+1] + \mathbf{e}[i]. \tag{5.1}$$

Notice that the diagonal terms of $\mathbf{A}$ represent the sub-channel gains, while the off-diagonal terms represent interference form other tones of the same block. Also the nonzero elements in $\mathbf{B}$ and $\mathbf{C}$ contribute to interblock interference. To facilitate our analysis, we write $\mathbf{A}$ as $\mathbf{A} = \mathbf{\Lambda} + \mathbf{A}_0$ where $\mathbf{\Lambda}$ is a diagonal matrix containing only the diagonal elements of $\mathbf{A}$ and $\mathbf{A}_0$ contains only the off-diagonal elements of $\mathbf{A}$. Then, we can write

$$\mathbf{u}[i] = \mathbf{\Lambda}\mathbf{s}[i] + \mathbf{A}_0\mathbf{s}[i] + \mathbf{B}\mathbf{s}[i-1] + \mathbf{C}\mathbf{s}[i+1] + \mathbf{e}[i]. \tag{5.2}$$

The elements of $\mathbf{A}$, $\mathbf{B}$ and $\mathbf{C}$ can be expressed in terms of the TEQ coefficients. In particular,

$$A_{kl} = \mathbf{a}_{kl}\mathbf{t},\;\; B_{kl} = \mathbf{b}_{kl}\mathbf{t},\;\; C_{kl} = \mathbf{c}_{kl}\mathbf{t}, \tag{5.3}$$

where $\mathbf{t}$ is the vector of TEQ coefficients. The derivations of the row vectors $\mathbf{a}_{kl}$, $\mathbf{b}_{kl}$ and $\mathbf{c}_{kl}$ are given in Appendix A. We would like design the TEQ such that interference from all these sources can be minimized. For instance, we can design the TEQ t_i such that a particular coefficient A_{k_0,l_0} is minimized. The term $|A_{k_0,l_0}|^2$ represent the interference from the l_0-th tone to the k_0-th tone. From Equation 5.3, we know $A_{k_0,l_0} = \mathbf{a}_{k_0,l_0}\mathbf{t}$. Therefore

$$|A_{k_0,l_0}|^2 = \mathbf{t}^\dagger \mathbf{a}_{k_0,l_0}^\dagger \mathbf{a}_{k_0,l_0}\mathbf{t},$$

which is a quadratic form of $\mathbf{t}$. The TEQ $\mathbf{t}$ that minimizes $|A_{k_0,l_0}|^2$ can be found by solving a eigen problem. Take VDSL test loop 7(sampling frequency $= 35.328MHz$) as an example. The impulse response of the channel is shown in Figure 5.1. We use $M = 8192$, $L = 640$ and $d = 0$. Suppose we choose $k_0 = 1500$ and $l_0 = 2000$. The equalized channel h_i in this case is shown in Figure 5.2. As a measure of shortening effect, we compute the SIR of the original channel and the equalized channel. The definition of SIR is as given in Equation 4.1. The SIR of the original and equalized channel are respectively $35.8dB$ and $59.4dB$. As second example, we choose $k_0 = 3500$ and $l_0 = 2500$. In Figure **??**, we show the two columns of $\mathbf{A}_0$, i.e., $|A_{0,k,l}|^2$ for $k = \{0, 1, \cdots, 4095\}$, $k \neq l$ where the two columns are $l = l_0 = 2000$ and $l = 100$. Although one tone interference from other one tone be minimized, ($|A_{0,k,l_0}|^2$ for $k = 4096, 4097, \cdots, 8191$ is not shown as each column of $\mathbf{A}_0$ is conjugate symmetric.) In Figure 5.4, we show the impulse response of equalized channel. The SIR of equalized channel is $58.04dB$. We can see that the channel si also successively shortened. Therefore minimizing one coefficients of $\mathbf{A}$ shortens the channel effectively. The reason for this is that the element A_{k_0,l_0} is a linear combination of equalized channel coefficients $h_0 \cdots h_{d-1}, h_{d+L} \cdots h_{N-1}$. Minimizing the $|\mathbf{A}_{k_0 l_0}|^2$ is implicitly minimizing the coefficients outside the windows and thus the channel is shortened. TEQ designed for minimizing the interference of one tone to another tone can effectively shorten the channel. Let us design TEQ for minimizing the several tones interference from several tones be considered. That is, let us minimize the elements in several columns of $\mathbf{A}$, $\mathbf{B}$ and $\mathbf{C}$. We design the TEQ by minimizing $\sum_{k\in\Xi}\sum_{l\in\Theta, l\neq k}|A_{k,l_0}|^2 + \sum_{k\in\Xi}\sum_{l\in\Theta}(|B_{k,l}|^2 + |C_{k,l}|^2)$ when Ξ and Θ are some chosen set of tones. As an example, we choose Ξ and $\Theta \in \{2500, \cdots, 4095\}$. The resulting equalized channel is shown in Figure 5.5.(a). The magnitude response of TEQ is shown in Figure 5.5.(b). The SIR of equalized channel is $72.43dB$. The equalized channel be successively shortening and the zeros of TEQ are mostly in the frequency band corresponding to Ξ and Θ. As another example, we choose the sets Ξ and $\Theta \in \{1500, \cdots, 2500\}$. The resulting equalized channel is shown in Figure 5.6.(a). The magnitude response of TEQ is shown in Figure 5.6.(b). The SIR of equalized

channel is $70.32dB$. The equalized channel is also shortening and zeros of TEQ is mostly in the frequency band corresponding to Ξ and Θ. To save the computation complexity, we will give two examples where the interference of one tone to several other tones of the same block and of different blocks be considered. That is, let us minimize several elements in the particular column of $\mathbf{A}$, $\mathbf{B}$ and $\mathbf{C}$. We design the TEQ by minimizing $\sum_{k\in\Xi} |A_{k,l_0}|^2 + |B_{k,l_0}|^2 + |C_{k,l_0}|^2$ when Ξ is some chosen set of tones. As an example, we choose $l_0 = 2500$ and $\Xi \in \{2501, \cdots, 4095\}$. The resulting equalized channel is shown in Figure 5.7.(a). The magnitude response of TEQ is shown in Figure 5.7.(b). The SIR of equalized channel is $58.98dB$. We can see that channel be shortened and zeros of TEQ are mostly in the frequency band corresponding to the tones in Ξ. As another example, the equalized channel and frequency response of TEQ by minimizing $\sum_{k\in\Xi} |A_{k,l_0}|^2 + |B_{k,l_0}|^2 + |C_{k,l_0}|^2$, we choose $\Xi \in \{1501, \cdots 2500\}$ and $l_0 = 1500$. The equalized channel is shown in Figure 5.8.(a). The SIR of equalized channel is $60.79dB$. The magnitude response of TEQ is shown in Figure 5.8.(b). We can see that channel be also shortened. The zeros of TEQ are also mostly in the frequency band corresponding to set Ξ. The TEQ design for minimizing one column elements has good channel shortening effect and the zeros of TEQ are both mostly in the frequency band corresponding to Ξ. The TEQ design can minimize one column elements of $\mathbf{A}$, $\mathbf{B}$ and $\mathbf{C}$ to save the computation complexity.

Remark. Intuitively, one natural cost function is the interference in the tones used for transmission, i.e., choosing Ξ to be the collection of used tones. However, as we have seen in the previous examples, the zeros of TEQ are mostly in the frequency band corresponding to Ξ. Choosing Ξ to be the collection of used tones will lead to TEQ with zeros in the used tones. This has an adverse effect on transmission rate. As a general guideline, we can choose unused tones for Ξ.

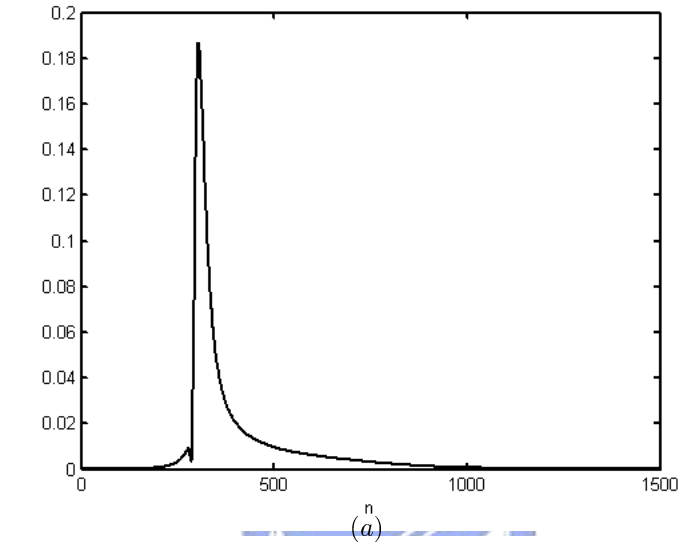

(a)

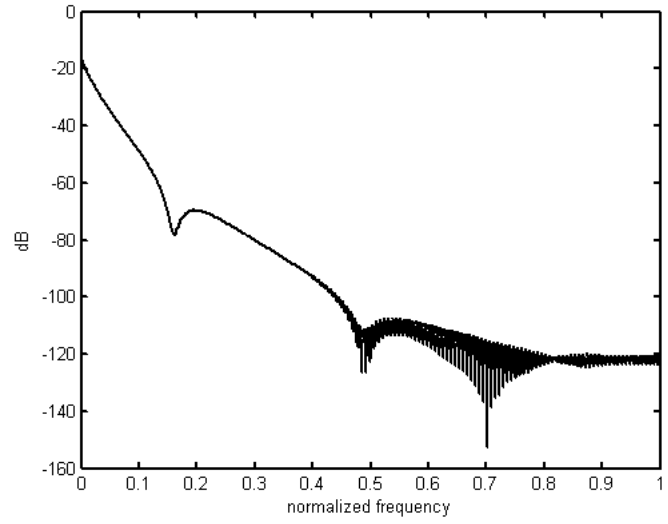

(b)

Figure 5.1: VDSL loop 7, (a) impulse response, (b) magnitude response.

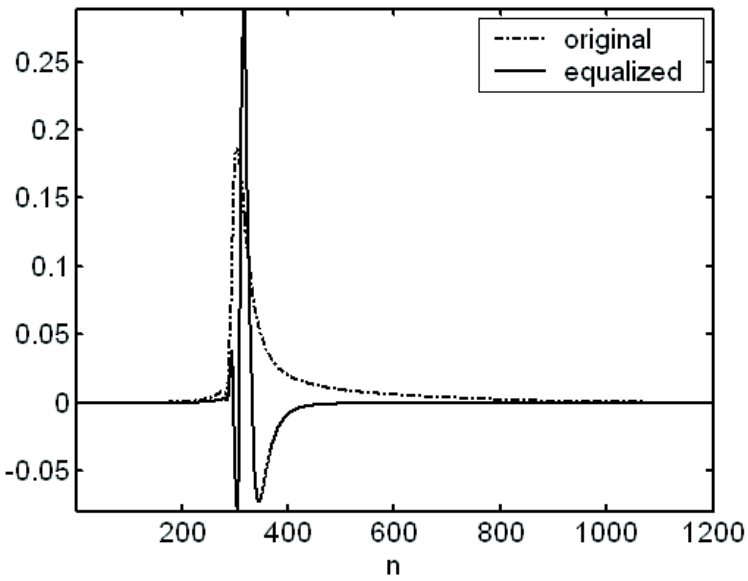

Figure 5.2: Impulse response of the original channel and equalized channel by minimizing $|A_{k_0 l_0}|^2$ with $k_0 = 1500$ and $l_0 = 2000$.

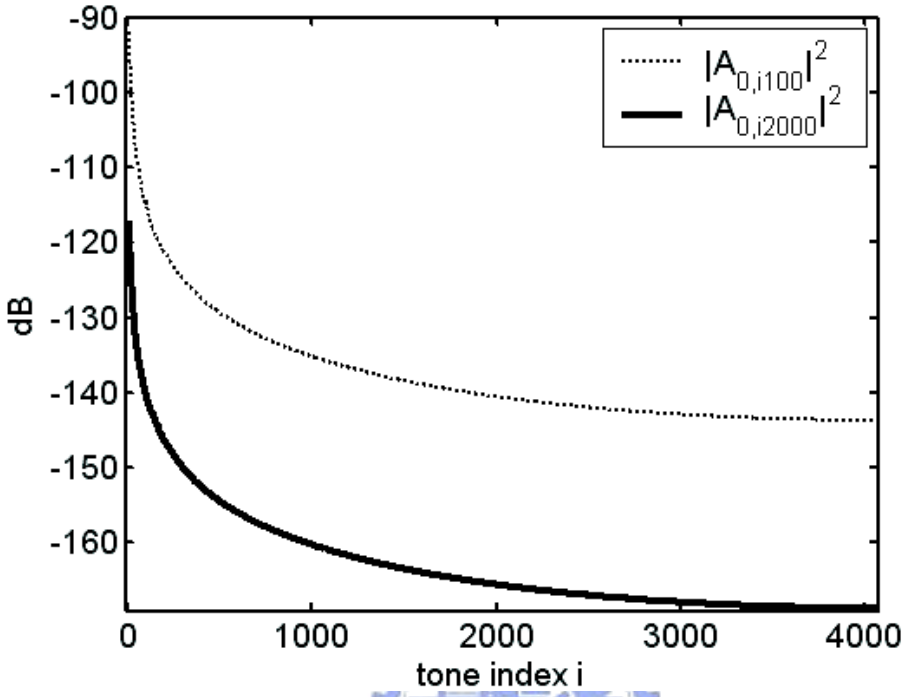

(*a*)

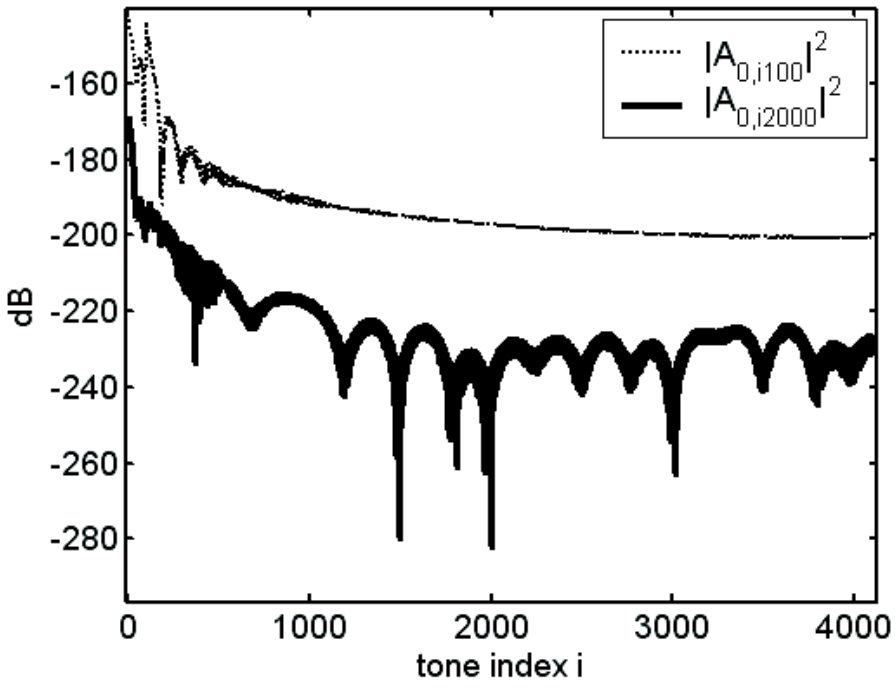

(*b*)

Figure 5.3: Columns of $\mathbf{A}_0$ (a) 100th column, (b) 2500th column.

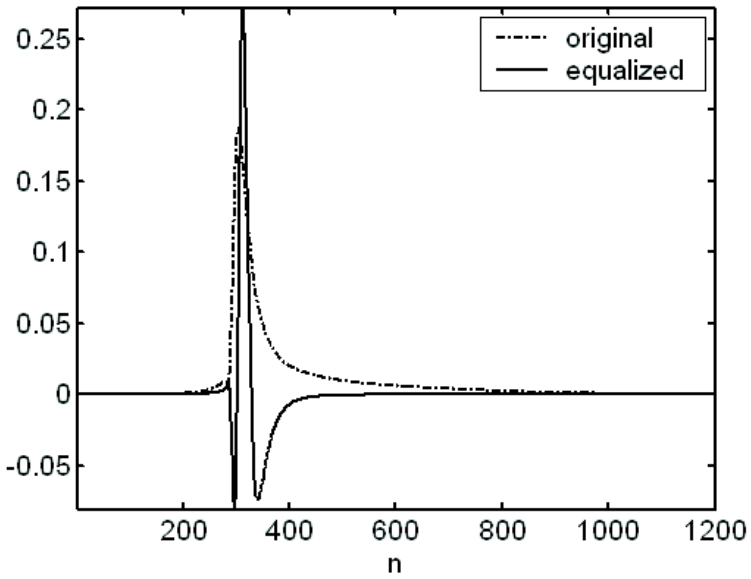

Figure 5.4: Impulse response of the original channel and equalized channel by minimizing $|A_{k_0 l_0}|^2$ with $k_0 = 3500$ and $l_0 = 2500$.

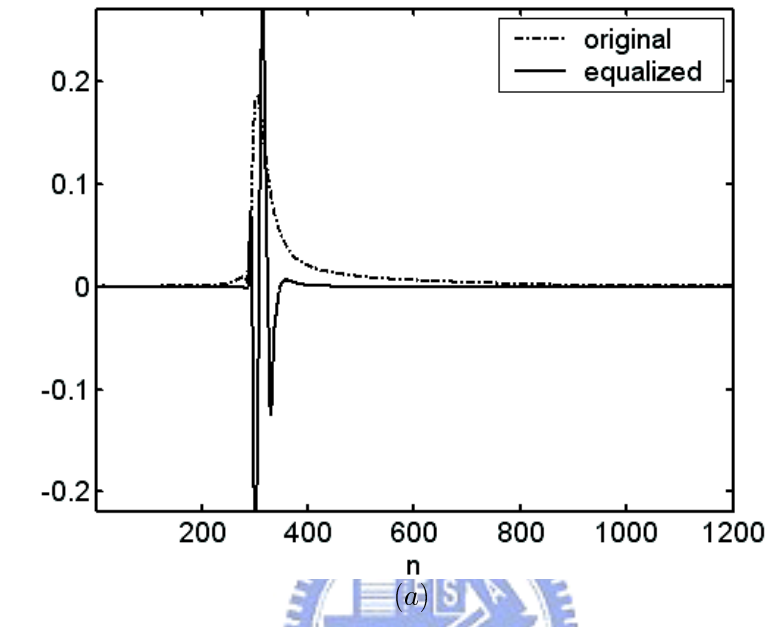

(a)

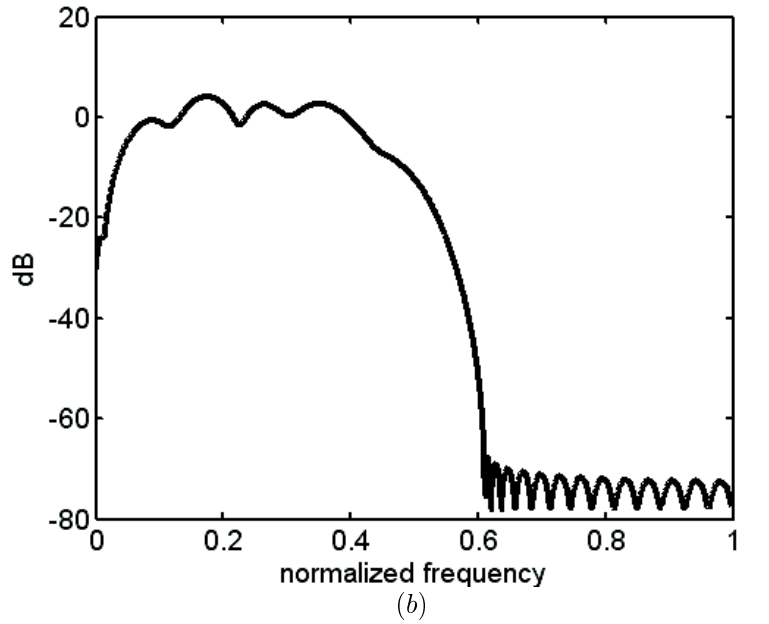

(b)

Figure 5.5: TEQ example on Ξ and $\Theta \in \{1500, 1501, \cdots, 2500\}$, (a) the original and equalized channel, (b) the magnitude response of TEQ.

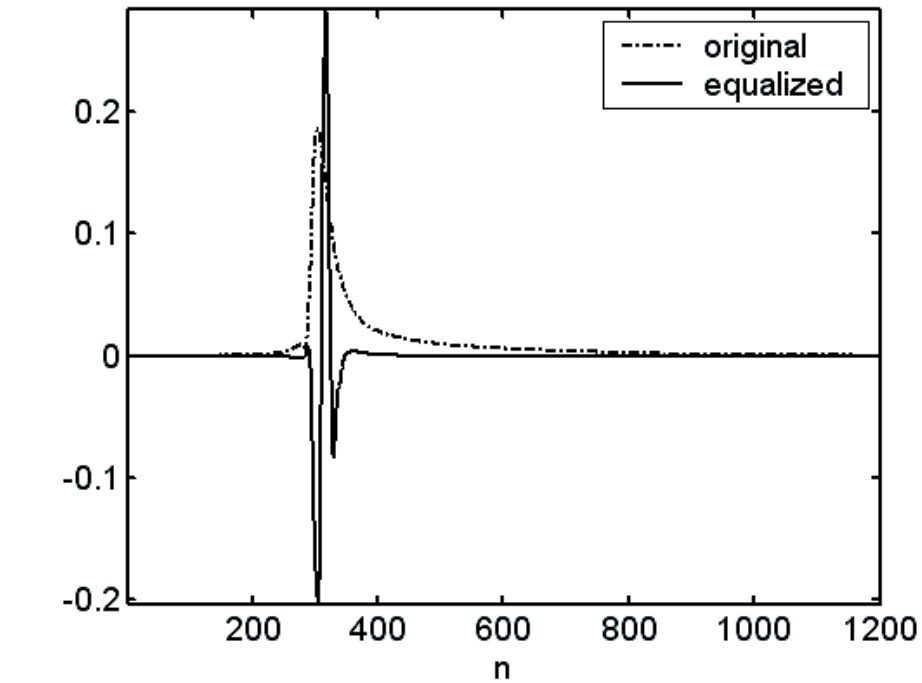

(a)

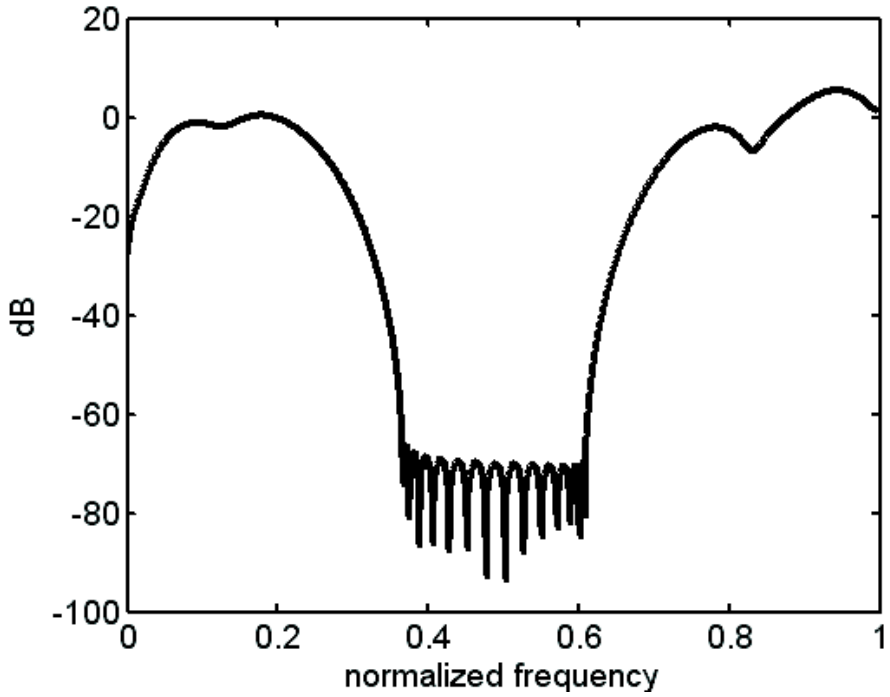

(b)

Figure 5.6: TEQ example on Ξ and $\Theta \in \{2500, 2501, \cdots, 4095\}$, (a) the original and equalized channel, (b) the magnitude response of TEQ.

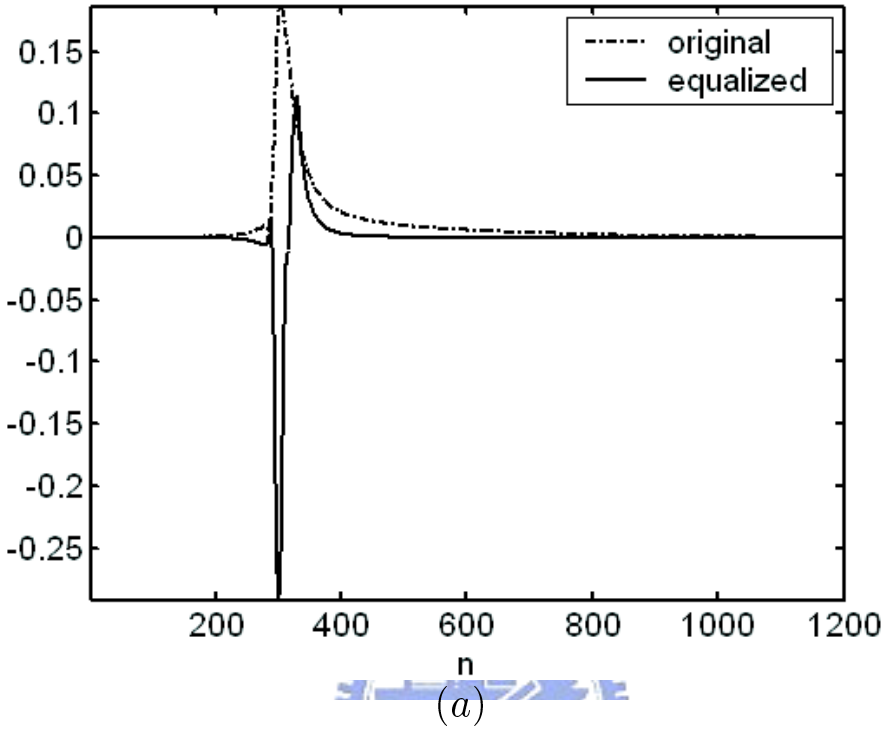

(a)

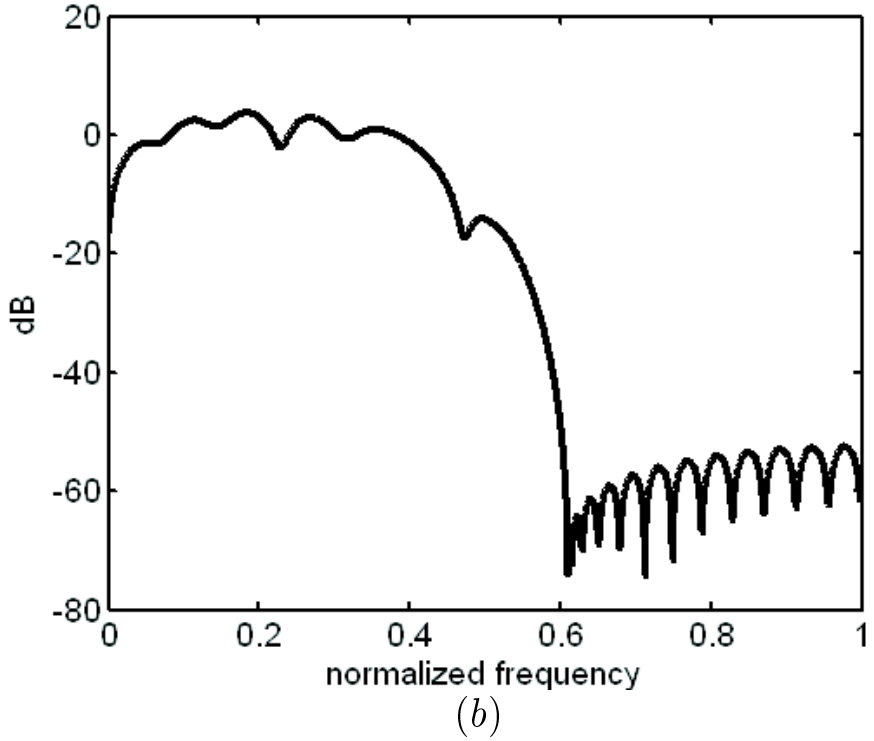

(b)

Figure 5.7: TEQ example on $\Xi \in \{2501, \cdots, 4096\}$ and $l_0 = 2500$, (a) the original and equalized channel, (b) the magnitude response of TEQ.

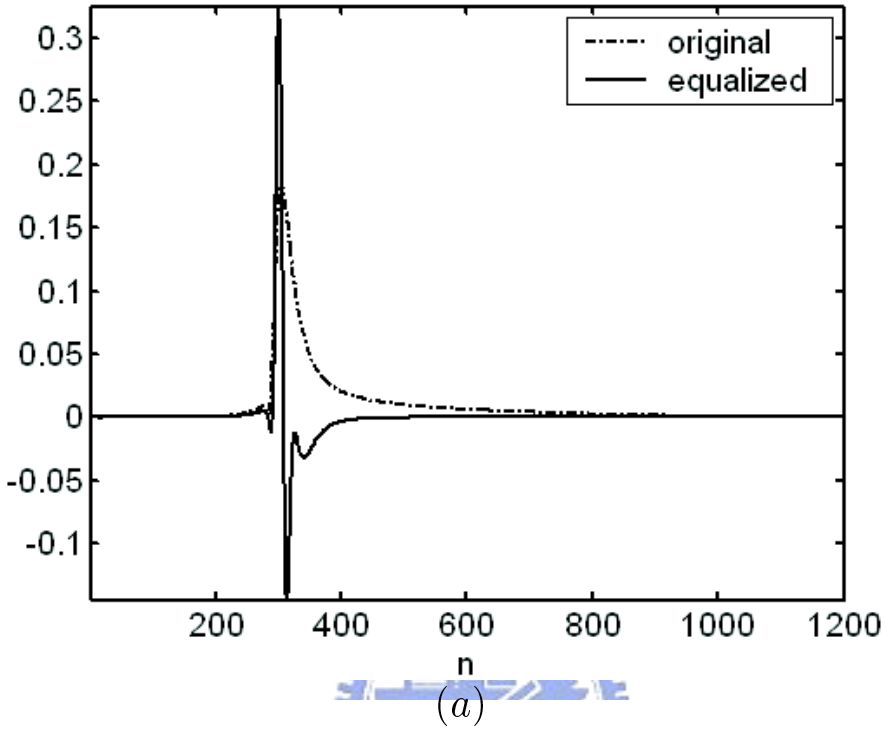

(a)

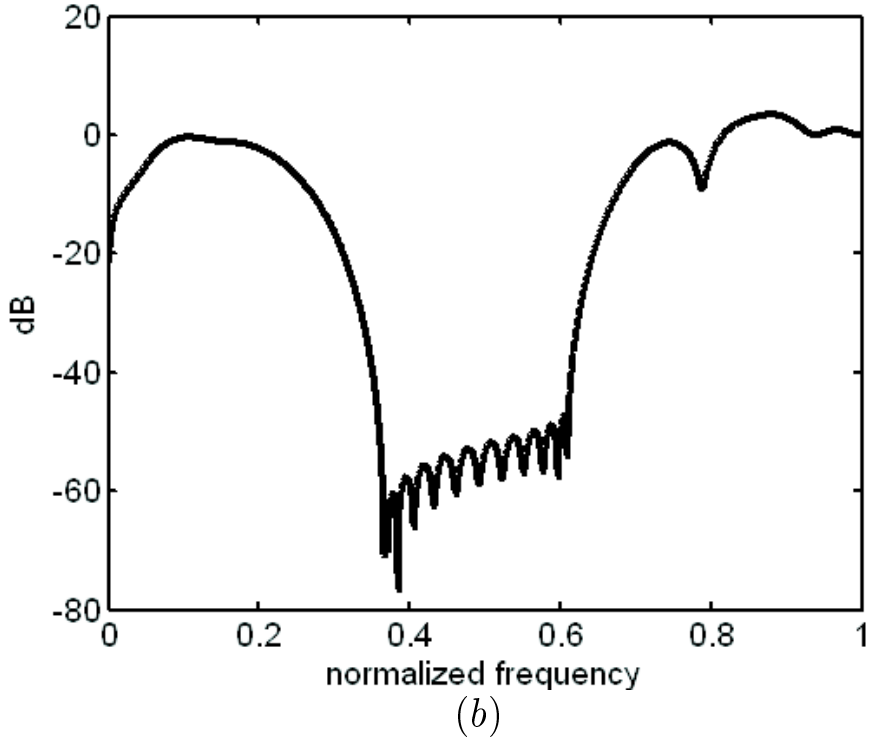

(b)

Figure 5.8: TEQ example on $\Xi \in \{1501, \cdots, 2500\}$ and $l_0 = 1500$, (a) the original and equalized channel, (b) the magnitude response of TEQ.

In light of the above examples, we propose the following cost function.

$$\min_{d} \quad \phi = \sum_{k\in\Xi}\sum_{l\in\Theta,l\neq k}|A_{kl}|^2 + \sum_{k\in\Xi}\sum_{l\in\Theta}|B_{kl}|^2 + |C_{kl}|^2, \tag{5.4}$$

where Θ denotes the set of tones whose interference to tones in Ξ will be minimized. From Equations A.8, A.14 and A.20, we have

$$A_{kl} = \mathbf{a}_{kl}\mathbf{t}, \quad B_{kl} = \mathbf{b}_{kl}\mathbf{t}, \quad C_{kl} = \mathbf{c}_{kl}\mathbf{t}, \tag{5.5}$$

where the elements of A_{kl}, B_{kl} and C_{kl} are all related to synchronization delay d. Then ϕ can be expressed as three parts,

$$\sum_{k\in\Xi}\sum_{l\in\Theta,l\neq k}|A_{kl}|^2 = \mathbf{t}^\dagger(\sum_{k\in\Xi}\sum_{l\in\Theta,l\neq k}\mathbf{a}_{kl}^\dagger\mathbf{a}_{kl})\mathbf{t}, \tag{5.6}$$

$$\sum_{k\in\Xi}\sum_{l\in\Theta}|B_{kl}|^2 = \mathbf{t}^\dagger(\sum_{k\in\Xi}\sum_{l\in\Theta}\mathbf{b}_{kl}^\dagger\mathbf{b}_{kl})\mathbf{t}, \tag{5.7}$$

$$\sum_{k\in\Xi}\sum_{l\in\Theta}|C_{kl}|^2 = \mathbf{t}^\dagger(\sum_{k\in\Xi}\sum_{l\in\Theta}\mathbf{c}_{kl}^\dagger\mathbf{c}_{kl})\mathbf{t}. \tag{5.8}$$

Let

$$\mathbf{A}_p = \sum_{k\in\Xi}\sum_{l\in\Theta,l\neq k}\mathbf{a}_{kl}^\dagger\mathbf{a}_{kl} + \sum_{k\in\Xi}\sum_{l\in\Theta}(\mathbf{b}_{kl}^\dagger\mathbf{b}_{kl} + \mathbf{c}_{kl}^\dagger\mathbf{c}_{kl})$$

Then the cost function ϕ becomes

$$\min_{d} \quad \phi = \mathbf{t}^\dagger\mathbf{A}_P\mathbf{t}, \tag{5.9}$$

which is a quadratic form of $\mathbf{t}$. It can be minimized by finding the eigenvector corresponding to the smallest eigenvalue of $\mathbf{A}_P$. The optimal TEQ $\mathbf{t}$ is obtain by exhaustively searching till the minimal cost function be found at a particular d.

Remark. Observing Figure 5.7.(b) and Figure 5.8.(b), we shall choose the successive tones for Ξ, Then most zeros will be in the tones belong to Ξ. The tones in the sets are chosen far away the used band for transmission and the most zeros be in the null tone band and keep the edge of used band for transmission on the height. For example, the proper sets for downstream transmission in VDSL are $\Xi = \{3001, 3002\cdots 4095\}$ and $\Theta = \{3000\}$. In this case, Ξ tones ISI from one tone $\Theta = \{3000\}$ be minimized.

Chapter 6

Numerical Simulation

In this chapter, the two performance measures used in our simulations, SIR and bit rate, will be introduced first in Section 6.1. Simulation environment is given in Section 6.2. A TEQ design example of the proposed method for VDSL loop 7 for downstream transmission are shown in Section 6.3. The results will be compared with those of MSSNR method. The performance of the proposed TEQ in terms of SIR is given in Section 6.4. Bit rate performance is given in Section 6.5. In the simulation results of Section 6.4 and 6.5, we will compare the proposed method TEQ with MSSNR [3] and MERRY [4].

6.1 Measures of Performance

We will use two performance measures:

- SIR: It is a good measure for evaluating channel shortening effect. The definition of SIR given in Equation 4.1 is repeated here.

$$\text{SIR} = \max_{d} \frac{\sum_{i=d}^{d+L} |h_i|^2}{\sum_{i=0, i\neq(d,\cdots d+L)}^{\nu} |h_i|^2}. \tag{6.1}$$

- Transmission rate: The number of bits allocated for the ith tone is

$$b_i = log_2(1 + \frac{\text{SINR}_\text{i}}{\eta}). \tag{6.2}$$

where $\mathrm{SINR_i}$ is the signal to interference and noise ratio of i-th tone. And η depends on desired error rate. For example, for an error rate of 10^{-5},η is 4.7863. Then the transmission rate is

$$\frac{1}{NT}\sum_{i=0}^{M/2} b_i. \tag{6.3}$$

For VDSL system, $M = 8192$, $L = 640$, $N = 8832$ and $\frac{1}{T} = 35.328MHz$. The maximum number of bits on each tone is 15.

6.2 Simulation Environment

We use VDSL as an example in our simulation [2]. The transmission media is twisted pair loop. The DFT size M is 8192, and cyclic prefix length L is 640. The sampling rate is $\frac{1}{T} = 35.328MHz$. The transmitted massage is mapped into QAM symbols. White Gaussian Noise (AWGN) with -170dBm/Hz and FEXT and NEXT noise are considered. The channel is assumed to be static. The loops used in our simulations are listed in Table 6.1. The magnitude response of the first 7 loops are shown in Figure 6.2.

Table 6.1: VSDL test loop length.

Loop	Length (feet)
VDSL-1L	4500
VDSL-2L	4750
VDSL-3L	4750
VDSL-4L	4800
VDSL-5	950
VDSL-6	3250
VDSL-7	4900
VDSL-1_2km	6562
VDSL-2_2km	6812
VDSL-3_2km	6812
VDSL-4_2km	6862

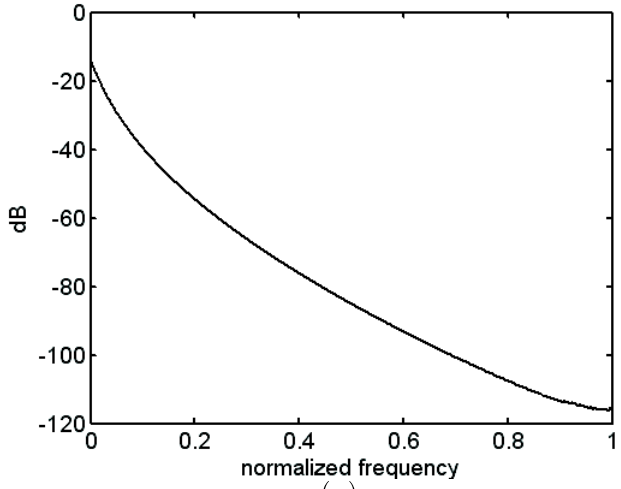
0
-20
-40
-60
-80
-100
-120
dB
0
0.2
0.4
0.6
0.8
1
normalized frequency
(a)

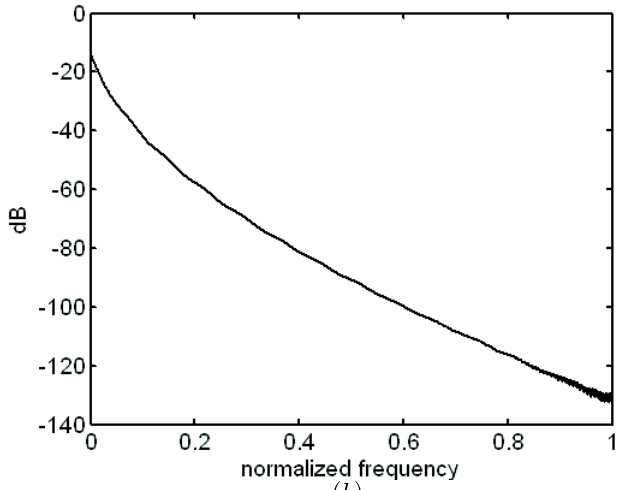
0
-20
-40
-60
-80
-100
-120
-140
dB
0
0.2
0.4
0.6
0.8
1
normalized frequency
(b)

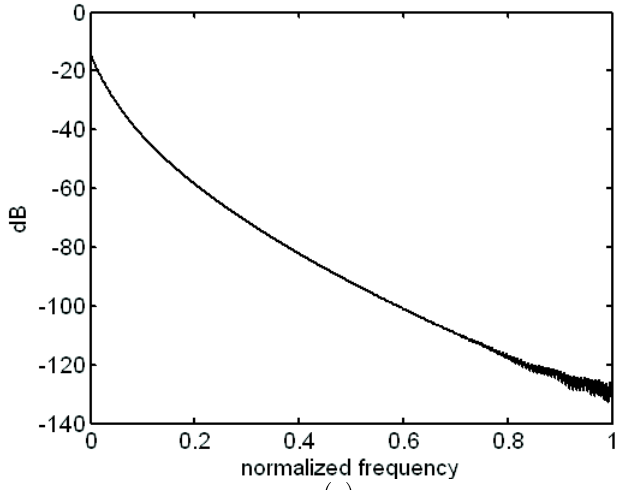
0
-20
-40
-60
-80
-100
-120
-140
dB
0
0.2
0.4
0.6
0.8
1
normalized frequency
(c)

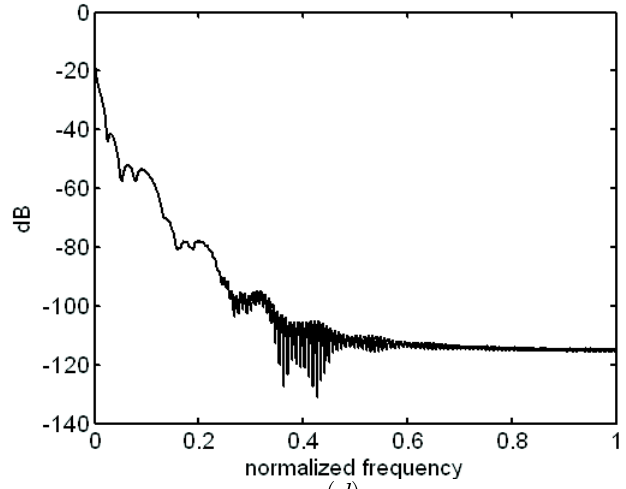
0
-20
-40
-60
-80
-100
-120
-140
dB
0
0.2
0.4
0.6
0.8
1
normalized frequency

(d)

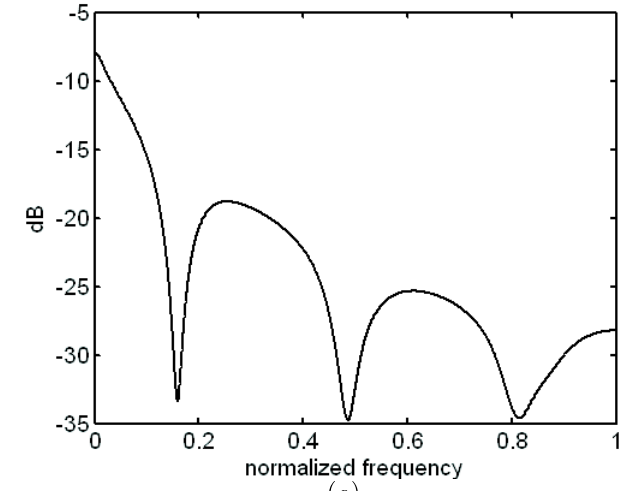
-5
-10
-15
-20
-25
-30
-35
dB
0
0.2
0.4
0.6
0.8
1
normalized frequency

(e)

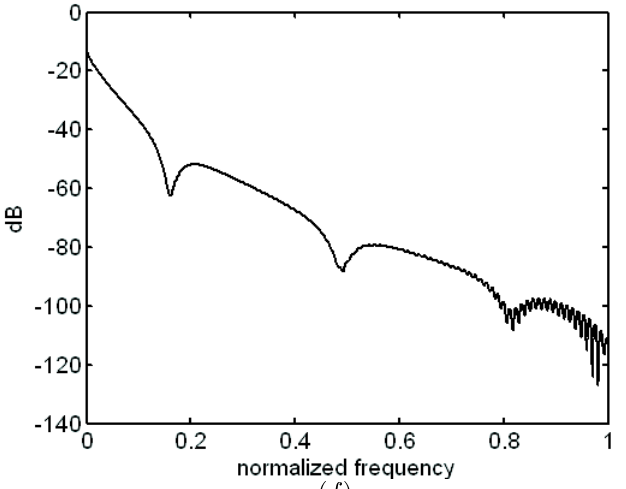
0
-20
-40
-60
-80
-100
-120
-140
dB
0
0.2
0.4
0.6
0.8
1
normalized frequency

(f)

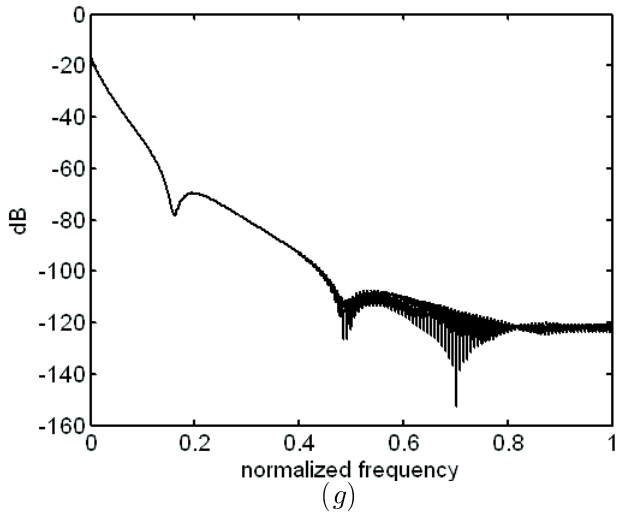

(g)

Figure 6.1: Magnitude responses of the First 7 test loops, (a) VDSL-1L, (b) VDSL-2L, (c) VDSL-3L, (d) VDSL-4L, (e) VDSL-5, (f) VDSL-6, (g) VDSL-7.

6.3 A TEQ Design Example

The channel used in this simulation is VDSL loop 7 of 4900 feet. The impulse response and frequency response of loop 7 are shown respectively in Figure 6.2(a) and 6.2(b). Downstrean transmission will be considered. We will design TEQ using the proposed method and MSSNR method. For the proposed method, we choose $\Xi = \{3001, 3002 \cdots 4095\}$ and $\Theta = \{3000\}$. The TEQ in both cases are of 40 taps. The impulse response of the two equalized channels are shown respectively in Figure 6.3(a) and 6.3(b). We can see that both TEQ have effective shortened the channel. The frequency response of the two TEQ are shown respectively in Figure 6.4(a) and 6.4(b). For the proposed method, the zeros of the TEQ are in the unused bands. The zeros of MSSNR TEQ are more uniformly distributed in both used and unused bands as shown in Figure 6.4(b). We plot for each individual tone signal power, interference, noise due to AWGN and noise due to crosstalk noise in Figure 6.5. Figure 6.6(a), (b), (c) shows respectively the bit loading for the case when there is no TEQ, the case with the proposed TEQ and the case with TEQ designed using MSSNR method. In Figure 6.6, we can see that both TEQ have better bit rate performance than the case without a TEQ. For the MSSNR method, dips occur around the zeros of the TEQ in the transmission band. This results in some loss in transmission rate.

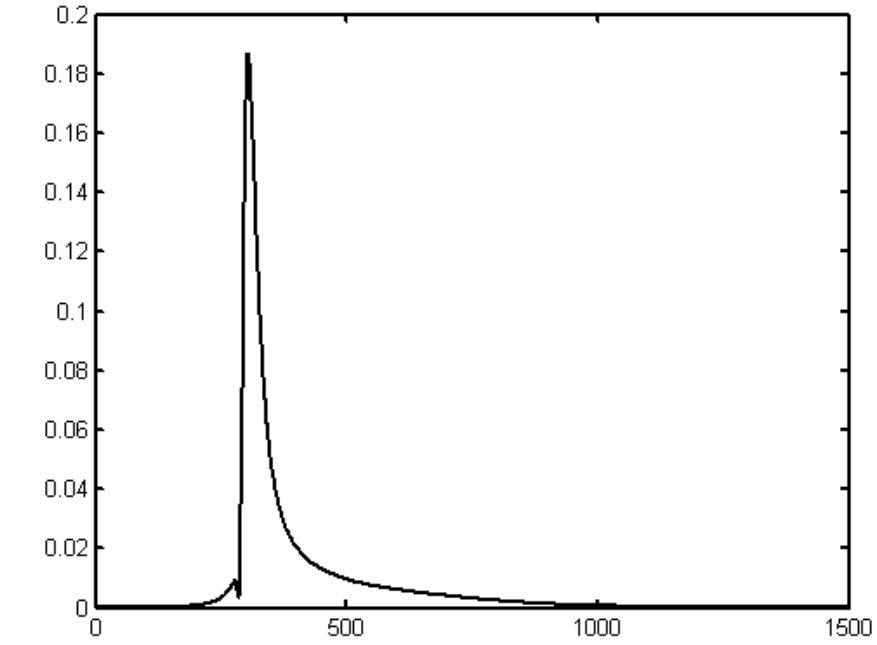

(a)

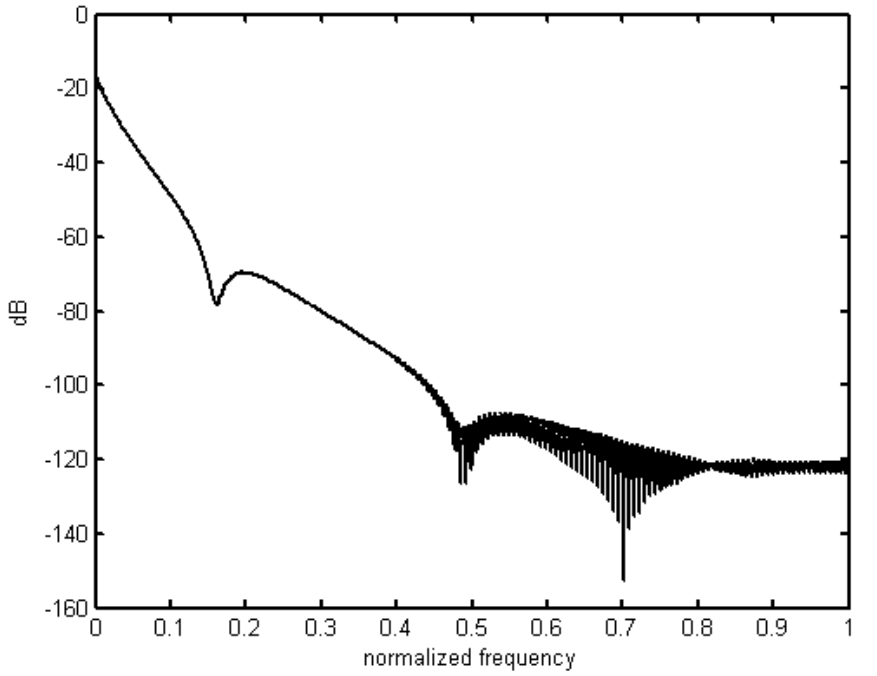

(b)

Figure 6.2: VDSL loop 7, (a) impulse response, (b) magnitude response.

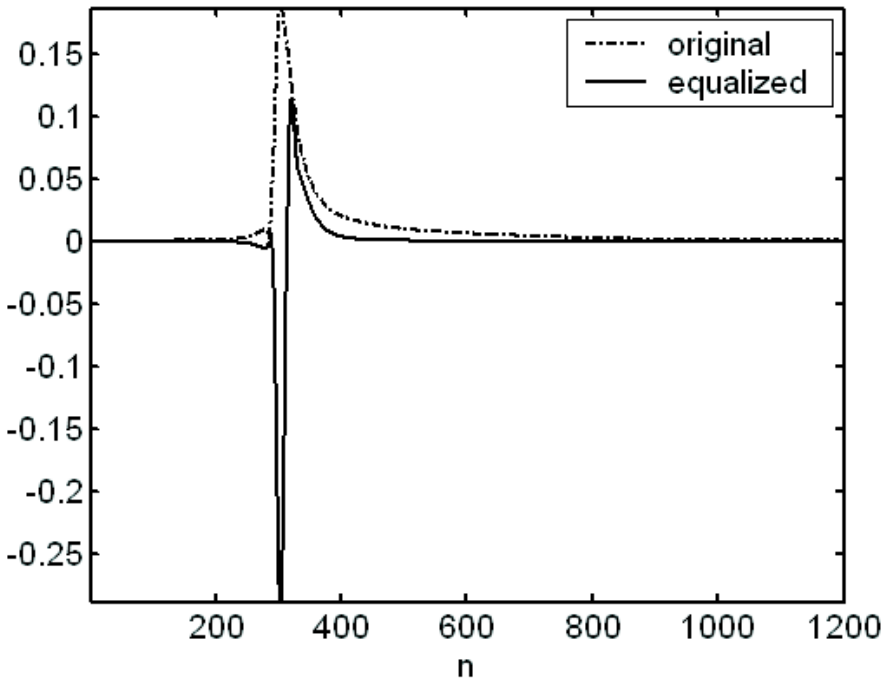

(a)

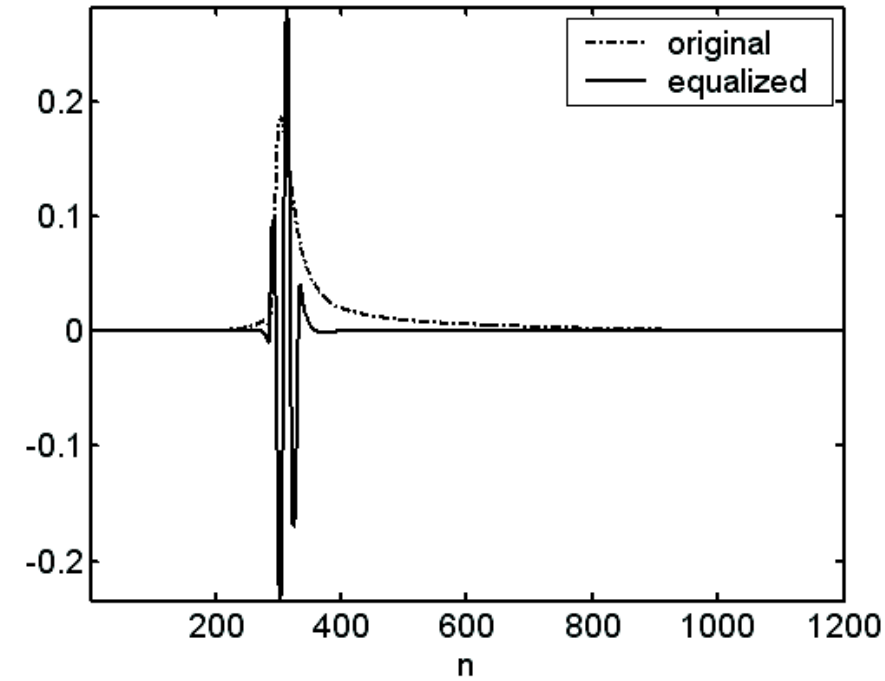

(b)

Figure 6.3: Impulse response of original channel and the equalized channel, (a) proposed method, (b) MSSNR.

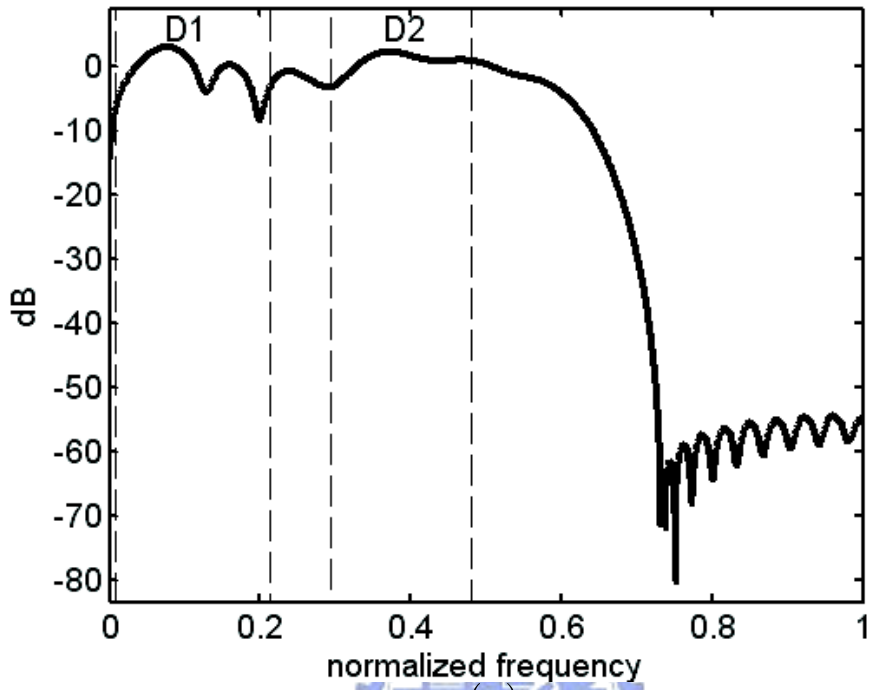

(a)

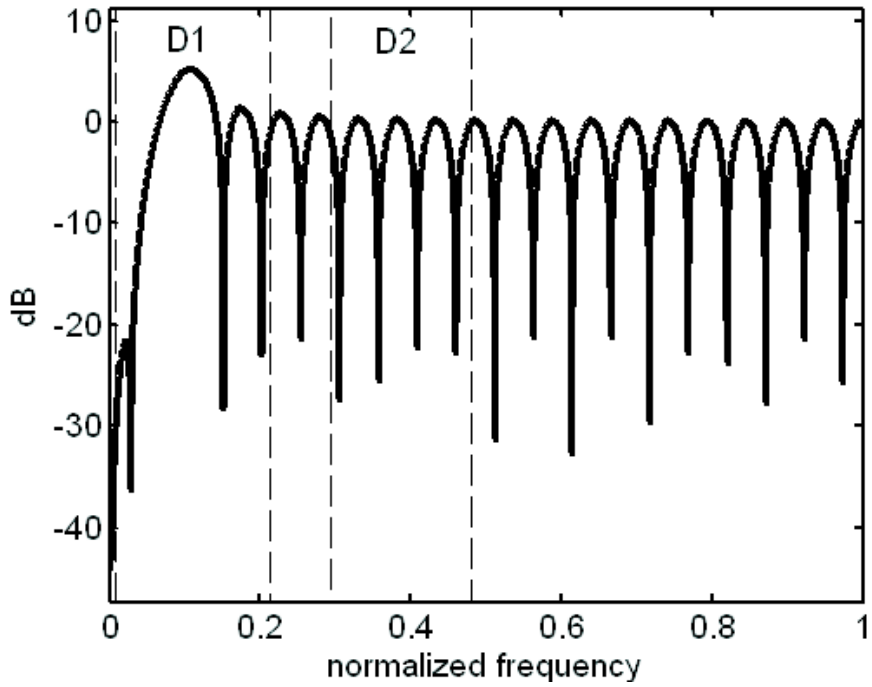

(b)

Figure 6.4: Frequency responses of TEQ, (a) proposed method, (b) MSSNR.

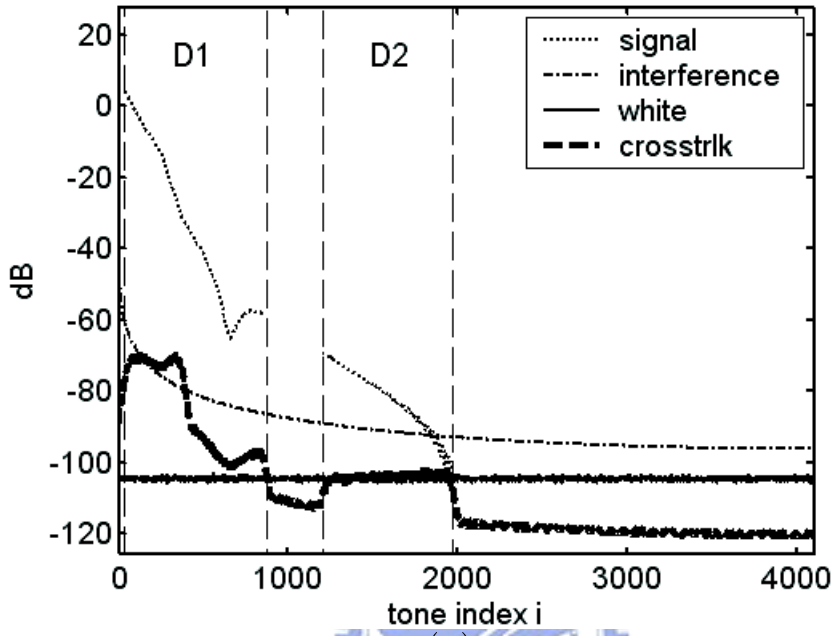
D1
D2
signal
interference
white
crosstrlk
dB
tone index i
20
0
-20
-40
-60
-80
-100
-120
0
1000
2000
3000
4000

(a)

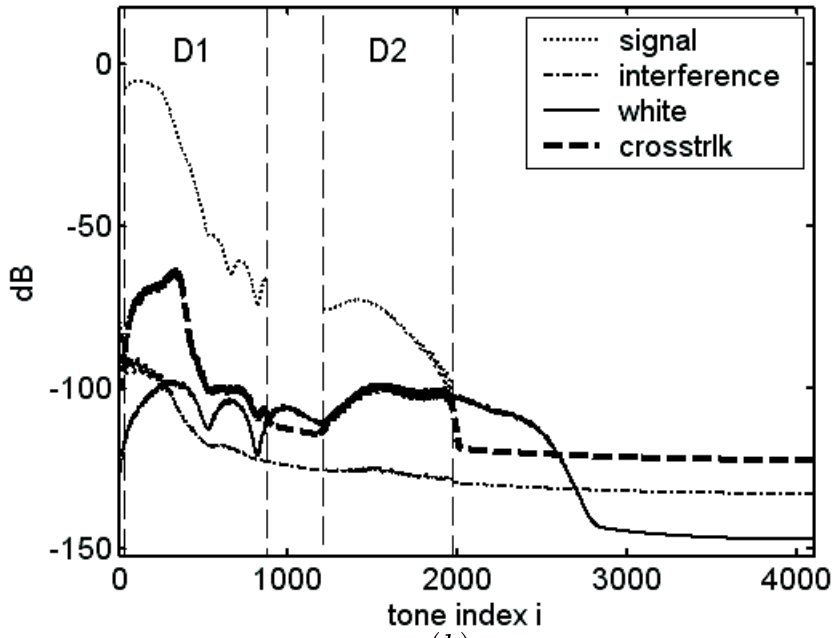
D1
D2
signal
interference
white
crosstrlk
dB
tone index i
0
-50
-100
-150
0
1000
2000
3000
4000

(b)

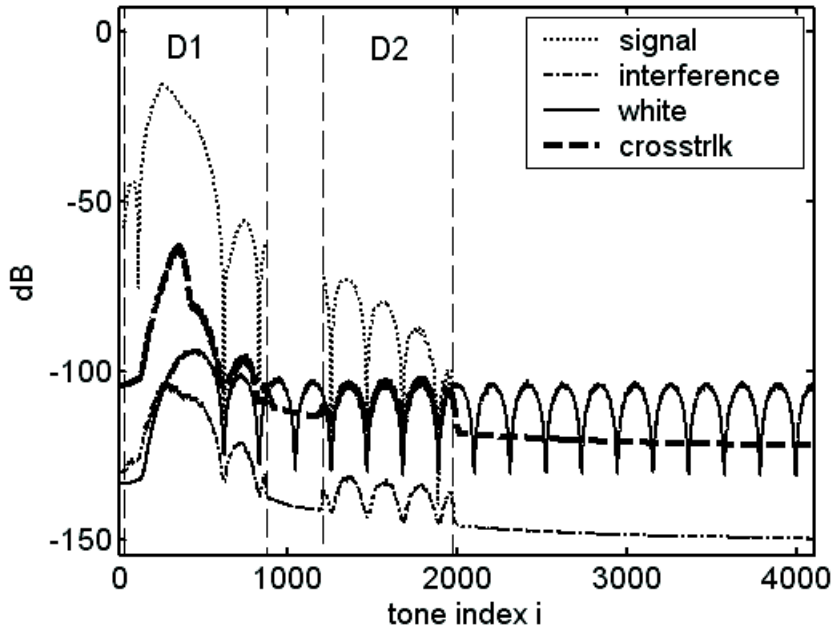

Figure 6.5: Signal, ISI and noise power in individual tone, (a) no TEQ case, (b) proposed method, (c) MSSNR.

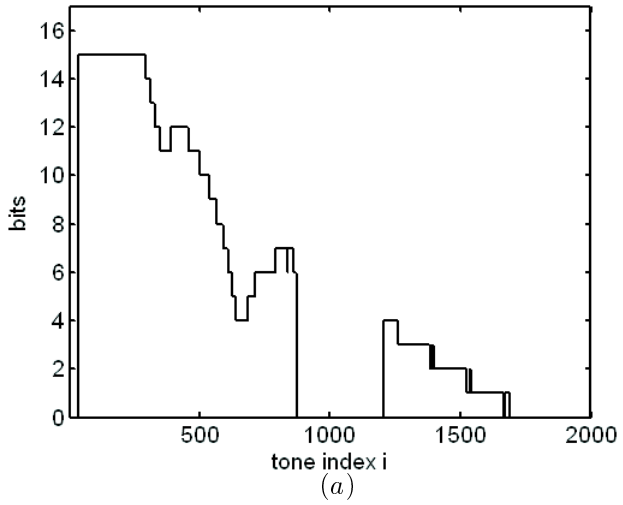

(a)

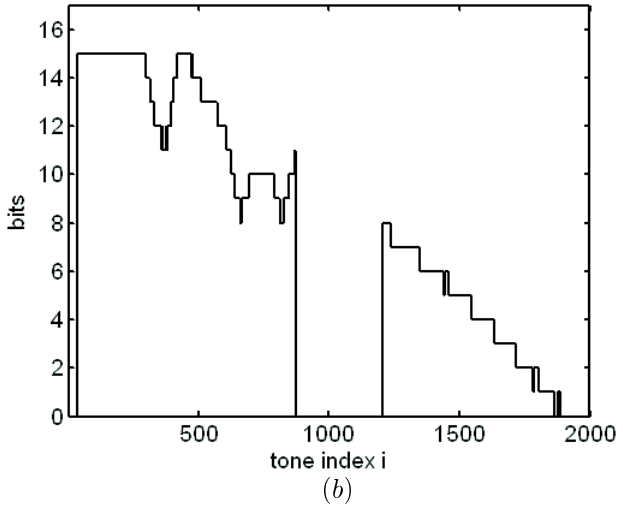

(b)

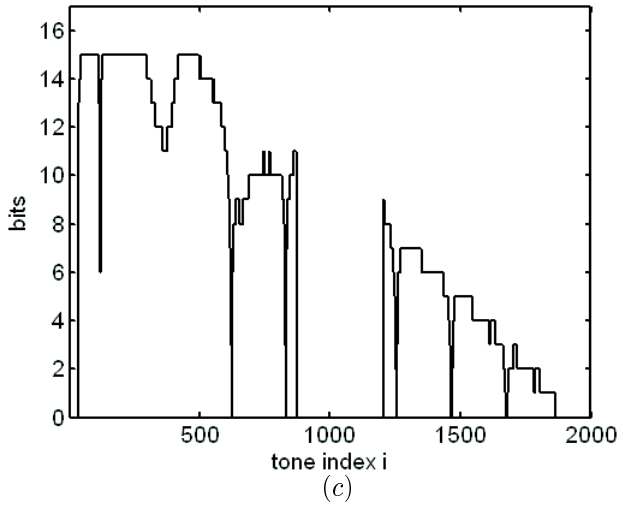

(c)

Figure 6.6: Bit loading, (a) no TEQ case, (b) proposed TEQ, (c) MSSNR.

6.4 SIR Performance

The SIR of the equalized channels with TEQ using our proposed method are listed in Table 6.2. The SIR of the original channels are also obtained by using Equation 6.2. For comparison, we have also listed the SIR of channel equalized using the MSSNR method [3], MERRY method [4] and MFSIR method [5] . All algorithm have the channel shortening effect. The MSSNR method has the largest SIR among the three. This is because the MSSNR method is optimal in the sense of maximal SIR.

Table 6.2: SIR (dB) on VDSL test loops.

Loop	Original channel	Proposed method	MSSNR	MERRY	MFSIR
VDSL-1L	47.68	83.19	101.17	54.02	80.69
VDSL-2L	49.86	71.87	91.10	53.94	72.08
VDSL-3L	43.36	85.84	90.55	50.31	67.64
VDSL-4L	28.63	52.18	67.10	35.57	61.22
VDSL-5	69.90	101.76	105.18	69.89	96.24
VDSL-6	53.01	91.85	94.98	58.28	69.46
VDSL-7	35.79	59.52	76.06	44.98	58.28
VDSL-1_2km	19.03	39.85	48.98	27.48	41.05
VDSL-2_2km	27.79	56.48	65.89	45.55	60.02
VDSL-3_2km	26.37	53.82	62.56	46.31	55.94
VDSL-4_2km	17.00	27.77	41.19	27.80	36.39

6.5 Transmission Rate Performance

The transmission rate performance of the proposed TEQ for all test loops in Table 6.7 is listed in Table 6.3, For comparison, we have also listed the transmission rates of MSSNR method, MERRY method, MFSIR method and the case when no TEQ is used. The transmission rate performance of proposed method is better than MSSNR and MERRY. For short loops, the TEQ is not important for transmission rate. In this case, no TEQ is better. For long loops, the TEQ can significantly enhances the bit rate performance. The bit rate performance for

VDSL loop 1 of different loop lengths is listed in Table 6.4 and plotted in Figure 6.7.

Table 6.3: Bit rate (Mbit/Sec) on VDSL test loops.

Loop	Original channel	Proposed method	MSSNR	MERRY	MFSIR
VDSL-1L	70.22	73.06	69.34	72.92	74.14
VDSL-2L	65.02	69.82	62.94	68.05	68.84
VDSL-3L	61.01	67.74	55.11	65.82	67.69
VDSL-4L	27.27	42.79	41.63	36.32	42.72
VDSL-5	94.26	94.18	90.92	94.25	92.15
VDSL-6	77.80	79.76	73.53	79.38	77.79
VDSL-7	39.39	54.17	53.01	49.42	54.71
VDSL-1_2km	15.46	27.8	25.03	22.86	27.16
VDSL-2_2km	29.71	42.26	40.87	40.3	42.00
VDSL-3_2km	29.12	41.34	39.97	39.74	40.85
VDSL-4_2km	10.22	16.97	16.01	16.08	16.73

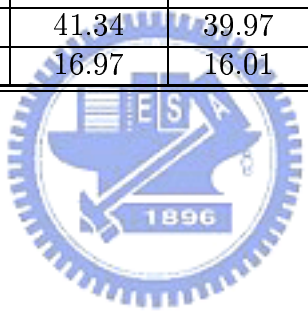

Table 6.4: Bit rate (Mbit/Sec) on VDSL loop 1 of different loop length.

Length (feet)	Original channel	Proposed method	MSSNR	MERRY	MFSIR
1000	94.03	94.06	90.79	94.04	93.98
1476	91.80	91.70	88.94	91.77	90.92
1969	90.07	89.91	85.19	90.04	90.00
2461	88.74	88.59	82.23	88.73	87.95
3000	86.73	86.63	81.74	86.76	86.66
3445	84.81	84.49	84.32	84.82	84.09
3937	80.23	79.68	76.91	80.64	80.24
4500	70.41	74.09	69.42	72.9	73.94
4921	59.00	67.37	63.09	64.85	67.92
5413	45.31	59.23	55.44	54.11	59.83
5906	37.48	52.65	44.76	44.84	52.504
6562	15.55	27.8	24.97	22.77	27.17

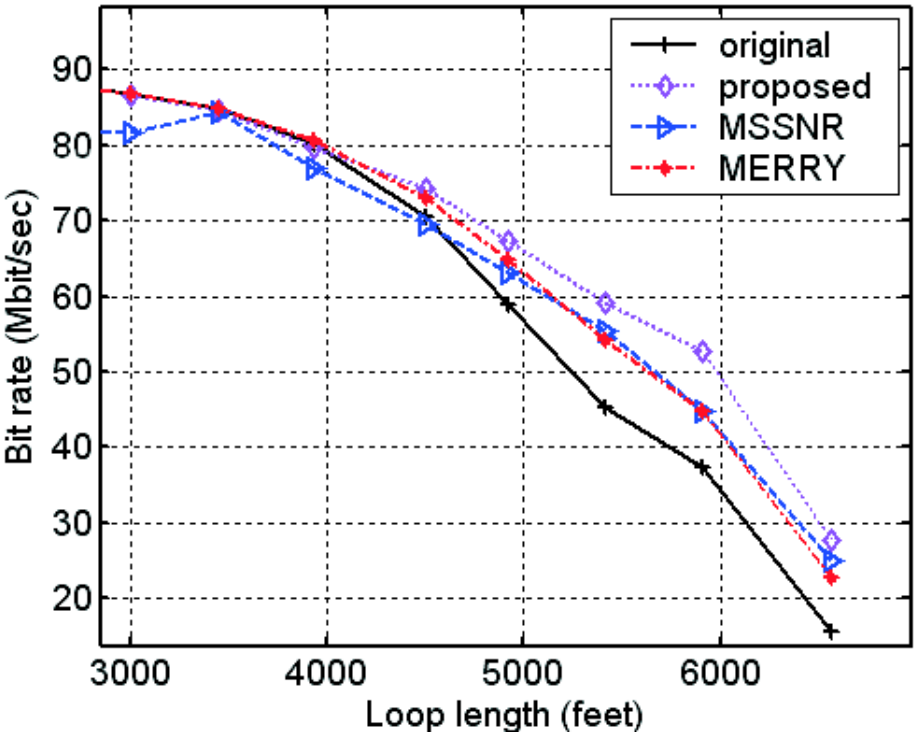

Figure 6.7: Bit rate for VDSL loop 1 of different loop length.

Conclusion

The channel will be ISI free if the channel order is smaller than the CP length. But the loops in DSL system are usually long and the channel order is larger than the CP length. The TEQ is needed to shorten the channel and mitigate ISI. The frequency response of TEQ also plays an important role in DSL system. The zeros in the transmission bands often results in a loss in bit rate. In this thesis, we minimize the interference in the frequency domain and observe the behavior of proposed TEQ. We can see that the proposed TEQ has the channel shortening effect and the zeros of TEQ be almost in the frequency corresponding to the tones which ISI be minimized. The simulation of VDSL system in downstream transmission is given in Chapter 6. We can see that all the test loops be shortened using the proposed TEQ. The zeros of proposed TEQ are almost in the null tone bands. The bit rate performance of proposed method is better than the MSSNR and MERRY method.

Appendix A

Elements of A, B and C Matrices

We will derive the elements of **A**, **B** and **C** in this appendix. From Equation 3.13 and **??**, the received output vector can be separated into 4 parts,

$$\mathbf{u}[i] = \mathbf{W}\mathbf{F}_1\mathbf{H}_0\mathbf{F}_0\mathbf{W}^\dagger\mathbf{s}[i] + \mathbf{W}\mathbf{F}_1\mathbf{H}_1\mathbf{F}_0\mathbf{W}^\dagger\mathbf{s}[i-1] + \mathbf{W}\mathbf{F}_1\mathbf{H}_2\mathbf{F}_0\mathbf{W}^\dagger\mathbf{s}[i+1] + \mathbf{e}[i]. \tag{A.1}$$

The matrix $\mathbf{H}_0$ can be expressed as $\mathbf{H}_{in}+\mathbf{H}_{out}$, where $\mathbf{H}_{in}$ depends on $h_d, h_{d+1}, \cdots, h_{d+L}$ and $\mathbf{H}_{out}$ depends on $h_0, \cdots, h_{d-1}, h_{D+L+1}, \cdots, h_{N-1}$ but not other coefficients. Then

$$\begin{aligned}\mathbf{u}[i] &= \underbrace{\mathbf{W}\mathbf{F}_1\mathbf{H}_{in}\mathbf{F}_0\mathbf{W}^\dagger}_{\mathbf{A}_{in}}\mathbf{s}[i] + \underbrace{\mathbf{W}\mathbf{F}_1\mathbf{H}_{out}\mathbf{F}_0\mathbf{W}^\dagger}_{\mathbf{A}_{out}}\mathbf{s}[i] + \underbrace{\mathbf{W}\mathbf{F}_1\mathbf{H}_1\mathbf{F}_0\mathbf{W}^\dagger}_{\mathbf{B}}\mathbf{s}[i-1] + \mathbf{e}[i] \\ &\quad + \underbrace{\mathbf{W}\mathbf{F}_1\mathbf{H}_2\mathbf{F}_0\mathbf{W}^\dagger}_{\mathbf{C}}\mathbf{s}[i+1] \\ &= \mathbf{A}_{in}\mathbf{s}[i] + \mathbf{A}_{out}\mathbf{s}[i] + \mathbf{B}\mathbf{s}[i-1] + \mathbf{C}\mathbf{s}[i+1] + \mathbf{e}[i]. \end{aligned} \tag{A.2}$$

The equalized channel coefficients, $h_i = c_i * t_i$, can be expressed as

$$\begin{bmatrix} h_0 \\ h_1 \\ \vdots \\ h_{N-1} \end{bmatrix} = \begin{bmatrix} c_0 & 0 & \cdots & 0 \\ c_1 & c_0 & \ddots & \vdots \\ \vdots & \ddots & & \vdots \\ c_\nu & \cdots & & c_{\nu-T_e+1} \\ \vdots & & \ddots & \vdots \\ c_{N+T_e-2} & \cdots & & c_{N-1} \end{bmatrix} \begin{bmatrix} t_0 \\ t_1 \\ \vdots \\ t_{T_e-1} \end{bmatrix}. \tag{A.3}$$

Notice that $c_i = 0, \forall i > \nu$, where ν is the channel order. Note that $\mathbf{F}_1\mathbf{H}_{in}\mathbf{F}_0$ is a circulant matrix,

$$\mathbf{F}_1\mathbf{H}_{in}\mathbf{F}_0 = \begin{bmatrix} h_d & 0 & \cdots & 0 & h_{d+L} & \cdots & h_{d+1} \\ h_{d+1} & d_d & \ddots & & 0 & \ddots & \vdots \\ \vdots & & \ddots & & & \ddots & h_{d+L} \\ h_{d+L} & h_{d+L-1} & & h_d & 0 & & 0 \\ 0 & h_{d+L} & & & \ddots & & \vdots \\ 0 & \cdots & 0 & h_{d+L} & h_{d+L-1} & \cdots & h_d \end{bmatrix}_{M\times M}. \quad \text{(A.4)}$$

The matrix $\mathbf{H}_{in}$ can be diagonalized using the DFT matrix and the diagonal terms are the M-point DFT of coefficients $h_d, h_{d+1} \cdots h_{d+L}$. The diagonal terms of $\mathbf{A}_{in}$ can be expressed as

$$\begin{aligned} A_{in,kk} &= \sum_{p=0}^{L} h(d+p) e^{-j\frac{2\pi}{M}kp} \\ &= \begin{bmatrix} e^{-j\frac{2\pi}{M}n\cdot 0} & \cdots & e^{-j\frac{2\pi}{M}n\cdot L} \end{bmatrix} \underbrace{\begin{bmatrix} c_d & \cdots & c_0 & 0 & \cdots & 0 \\ c_{d+1} & \cdots & & \ddots & \ddots & \vdots \\ & & & & \ddots & 0 \\ \vdots & & & & \ddots & c_0 \\ & & & & & \vdots \\ c_{d+L} & c_{d+L-1} & \cdots & & & c_{d+L-T+1} \end{bmatrix}}_{\mathbf{P}_1} \mathbf{t} \\ &= \begin{bmatrix} e^{-j\frac{2\pi}{M}n\cdot 0} & \cdots & e^{-j\frac{2\pi}{M}n\cdot L} \end{bmatrix} \mathbf{P}_1\mathbf{t}. \end{aligned} \quad \text{(A.5)}$$

We can derive the coefficients of $\mathbf{A}_{out}$ in a step by step manner.

$$\mathbf{A}_{out} = \mathbf{W}\mathbf{F}_1\mathbf{H}_{out}\mathbf{F}_0\mathbf{W}^\dagger$$

$$= \mathbf{W} \begin{bmatrix} 0 & h_{d-1} & \cdots & h_0 & 0 & \cdots & 0 & & 0 \\ & & h_{d-1} & & \ddots & h_{d+L+1} & & \ddots & \vdots \\ & & & \ddots & & \vdots & & & 0 \\ \vdots & & & & & h_0 + h_{M-2d} & & & h_{d+L+1} \\ & & \ddots & & & \vdots & & & \vdots \\ & & & 0 & & h_{d-1} + h_{M+d-1} & & & h_{M-2d-1} \\ 0 & & & & \ddots & \vdots & & & h_0 + h_{M-2d} \\ h_{d+L+1} & 0 & & & & h_{N-1} & & & \vdots \\ \vdots & \ddots & & \ddots & & & & \ddots & h_{d-1} + h_{M+d-1} \\ h_{M+d-1} & \cdots & & h_{d+L+1} & 0 & 0 & h_{N-1} & \cdots & h_{M+d} \end{bmatrix} \mathbf{W}^\dagger$$

$$= \mathbf{W}\boldsymbol{\Upsilon}. \tag{A.6}$$

The element of $\boldsymbol{\Upsilon}$ is

$$\Upsilon_{kl} = \begin{cases} \frac{1}{\sqrt{M}} \sum_{i=1}^{d} h_{d-i} e^{j\frac{2\pi il}{M}}, & k = 0 \\ \frac{1}{\sqrt{M}} (\sum_{i=1}^{d} h_{d-i} e^{j\frac{2\pi(i+k)l}{M}} + \sum_{i=1}^{k} h_{d+L+k-i+1} e^{j\frac{2\pi(M-L+i-1)l}{M}}), & 1 \le k \le M-d-1 \\ \frac{1}{\sqrt{M}} (\sum_{i=1}^{M-k-1} h_{d-i} e^{j\frac{2\pi(i+k)l}{M}} + \sum_{i=k-M+d+2}^{k} h_{d+L+k-i+1} e^{j\frac{2\pi(M-L+i-1)l}{M}}), & M-d \le k \le M-2 \\ \frac{1}{\sqrt{M}} \sum_{i=d+1}^{M-1} h_{N+d-i} e^{j\frac{2\pi(M-L+i-1)l}{M}}, & k = M-1 \end{cases} \tag{A.7}$$

Then the elements of $\mathbf{A}_{out}$ is given by $A_{out,kl} = \frac{1}{\sqrt{M}} \sum_{i=0}^{M-1} \Upsilon_{il} e^{-j\frac{2\pi ki}{M}}$. They can be expressed as

$$\begin{aligned} A_{out,kl} &= \tilde{\mathbf{z}}_{kl} \underbrace{\begin{bmatrix} c_0 & 0 & \cdots & & 0 \\ \vdots & \ddots & \ddots & & \vdots \\ c_{d-1} & \cdots & c_0 & 0 \cdots & 0 \\ c_{d+L+1} & c_{d+L} & \cdots & & c_{d+L-T+2} \\ \vdots & & \ddots & & \vdots \\ c_{N-1} & c_{N-2} & \cdots & & c_{N-T} \end{bmatrix}}_{\mathbf{P}_2} \mathbf{t} \\ &= \tilde{\mathbf{z}}_{kl} \mathbf{P}_2 \mathbf{t}, \end{aligned} \tag{A.8}$$

when

$$\tilde{\mathbf{z}}_{kl} = \begin{bmatrix} \tilde{z}_0 & \tilde{z}_1 & \cdots & \tilde{z}_{M-2} \end{bmatrix}_{1\times(M-1)}, \tag{A.9}$$

with

$$\tilde{z}_i = \begin{cases} \frac{1}{M} \sum_{m=0}^{M-d+i-1} e^{-j\frac{2\pi km}{M}} e^{j\frac{2\pi(m+d-i)l}{M}}, & 0 \le i \le d-1 \\ \frac{1}{M} \sum_{m=i-d+1}^{M-1} e^{-j\frac{2\pi km}{M}} e^{j\frac{2\pi(m-L+d-i-1)l}{M}}, & d \le i \le M-2 \end{cases} \tag{A.10}$$

$$\mathbf{a}_{kl} = \tilde{\mathbf{z}}_{kl} \mathbf{P}_2 \quad \text{for } k \ne l. \tag{A.11}$$

The matrix $\mathbf{B}$ in Equation A.2 can be simplified as

$$\mathbf{B} = \mathbf{W} \begin{bmatrix} 0 & \cdots & 0 & h_{N-1} & \cdots & h_{d+L+1} \\ & & & & \ddots & \vdots \\ & & & \ddots & & h_{N-1} \\ \vdots & & & & & 0 \\ & & & & & \vdots \\ 0 & & & \cdots & & 0 \end{bmatrix} \mathbf{W}^{\dagger}$$

$$= \mathbf{W}\boldsymbol{\Psi}. \tag{A.12}$$

The element of $\boldsymbol{\Psi}$ is

$$\Psi_{kl} = \begin{cases} \frac{1}{\sqrt{M}} \sum_{i=d+1+k}^{M-1} h_{N+d+k-i} e^{j\frac{2\pi il}{M}}, & 0 \le k \le M-d-2 \\ 0, & M-d-1 \le k \le M-1 \end{cases} \tag{A.13}$$

Then, the elements of $\mathbf{B}$ is given by $B_{kl} = \frac{1}{\sqrt{M}} \sum_{i=0}^{M-1} \Psi_{il} e^{-j\frac{2\pi ki}{M}}$, can be expressed as

$$\begin{aligned} B_{kl} &= \tilde{\mathbf{r}}_{kl} \underbrace{\begin{bmatrix} c_{d+L+1} & \cdots & c_{d+L+T-2} \\ c_{d+L+2} & \cdots & c_{d+L+T-1} \\ \vdots & \ddots & \vdots \\ c_{N-1} & \cdots & c_{N-T} \end{bmatrix}}_{\mathbf{P}_3} \mathbf{t} \\ &= \tilde{\mathbf{r}}_{kl} \mathbf{P}_3 \mathbf{t}, \end{aligned} \tag{A.14}$$

when

$$\tilde{\mathbf{r}}_{kl} = [\, \tilde{r}_0 \quad \tilde{r}_1 \quad \cdots \quad \tilde{r}_{M-d-2} \,]_{1\times(M-d-1)} \tag{A.15}$$

with

$$\tilde{r}_i = \frac{1}{M} \sum_{m=0}^{i} e^{-j\frac{2\pi km}{M}} e^{j\frac{2\pi(m-i-1)l}{M}}. \tag{A.16}$$

$$\mathbf{b}_{kl} = \tilde{\mathbf{r}}_{kl} \mathbf{P}_3. \tag{A.17}$$

The matrix $\mathbf{C}$ can be simplified as

$$\begin{aligned} \mathbf{C} &= \mathbf{W} \begin{bmatrix} 0 & \cdots & 0 & & \cdots & 0 \\ \vdots & & & & & \vdots \\ 0 & & & \ddots & & \\ h_0 & & \ddots & & & 0 \\ \vdots & \ddots & & & & \vdots \\ h_{d-1} & \cdots & h_0 & 0 & \cdots & 0 \end{bmatrix} \mathbf{W}^{\dagger} \\ &= \mathbf{W}\boldsymbol{\Omega}. \end{aligned} \tag{A.18}$$

The elements of $\boldsymbol{\Omega}$ are given by

$$\Omega_{kl} = \begin{cases} 0, & 0 \le k \le M-d-1 \\ \frac{1}{\sqrt{M}} \sum_{i=M-d}^{k} h_{k-i} e^{j\frac{2\pi(m+d-L)l}{M}}, & M-d \le k \le M-1 \end{cases} \tag{A.19}$$

Then, the elements of $\mathbf{C}$ is $C_{kl} = \frac{1}{\sqrt{M}} \sum_{i=0}^{M-1} \Omega_{il} e^{-j\frac{2\pi ki}{M}}$. They can be expressed as

$$\begin{aligned} C_{kl} &= \tilde{\mathbf{o}}_{kl} \underbrace{\begin{bmatrix} c_0 & 0 & \cdots & 0 \\ \vdots & \ddots & \ddots & \vdots \\ c_{d-1} & \cdots & c_0 & 0 & \cdots & 0 \end{bmatrix}}_{\mathbf{P}_4} \mathbf{t} \\ &= \tilde{\mathbf{o}}_{kl} \mathbf{P}_4 \mathbf{t}, \end{aligned} \tag{A.20}$$

when

$$\tilde{\mathbf{o}}_{kl} = \begin{bmatrix} \tilde{o}_0 & \tilde{o}_1 & \cdots & \tilde{o}_{d-1} \end{bmatrix}_{1\times d}, \tag{A.21}$$

with

$$\tilde{o}_i = \frac{1}{M} \sum_{m=M-d+i}^{M-1} e^{-j\frac{2\pi km}{M}} e^{j\frac{2\pi(m+d-L-i)l}{M}} \tag{A.22}$$

$$\mathbf{c}_{kl} = \tilde{\mathbf{o}}_{kl} \mathbf{P}_4. \tag{A.23}$$

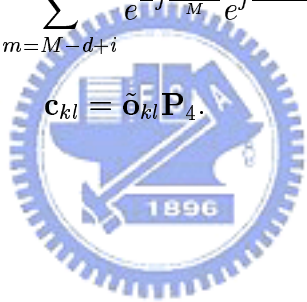

Bibliography

[1] *Asymmetric Digital Subscriber Lines (ADSL)-Metallic Interface*, ANSI T1.413, 1998.

[2] *Very-high Speed Digital Subscriber Lines (VDSL)-Metallic Interface*, ANSI T1.424, 2002.

[3] P. J. W. Melsa, R. C. Younce, and C. E. Rohrs,"Impulse response Shortening for Discrete Multitone Transceivers", *IEEE Trans. on Communication*, Vol. 44, no.12, pp.1662-1672, DEC.1996.

[4] R. K. Martin, J. Balakrishnan, W. A. Sethares, and C. R. Jr. Johnson,"Blind, adaptive channel shortening for multicarrier systems", *Signals, Systems and Computers, 2002. Conference Record of Thirty-sixth Asilomar Conference*, Vol. 1, pp.372-376, NOV.2002.

[5] Li-Han Liang"Design of Time Domain Equalizer (TEQ) for VDSL system", *Thesis of National Chiao Tung University*, JUN.2004.

[6] J. Balakrishnan, R. K. Martin, and C. R. Jr. Johnson"Blind, adaptive channel shortening by sum-square auto-correlation minimization (SAM)", *IEEE Trans. on Signal Processing*, pp.3086-3093, DEC.2003.

[7] G. Arslan, B. L. Evans, S. Kiaei,"Equalization for Discrete Multitone Transceivers to Maximize Bit Rate", *IEEE Trans. on Signal Processing*, Vol. 49, DEC.2001.

[8] Chun-Yang Chen and See-May Phoong,"Bit Rate Optimized Time-Domain Equalizers for DMT Systems", *Proc. of the 2003 International Symposium*, Vol. 4, pp.IV-37 - IV-40, MAY.2003.

[9] B. Farhang-Boroujeny and M. Ding,"Design Method for Time-Domain Equalizers in DMT Transceivers", *IEEE Trans. on Communication*, Vol. 49, no.3, pp.554-562, MAR.2001.

[10] A. V. Oppenhelm, R. W. Schafer, and J. R. Buck, *Discrete-Time Signal Processing*, Prentice-Hall, 1998.

[11] I. Djokovic,"MMSE Equalizers for DMT Systems with and without Crosstalk", *Signals, Systems and Computers, 1997. Conference Record of the Thirty-First Asilomar Conference*, Vol.1, pp.545 -549, 1998.

[12] M. de Courville, P. Duhamel, P. Madec and Palicot,"Blind Equalization of OFDM System Based on the Minimization of a Quadraic Criterion", *Proceedings of the Int. Conf. on Communications*, Dallas, TX, JUN.1996.